Soft Matter

PAPER

Cite this: *Soft Matter*, 2023, **19**, 208

The effective shear modulus of a random isotropic suspension of monodisperse liquid *n*-spheres: from the dilute limit to the percolation threshold†

Kamalendu Ghosh,[a] Victor Lefèvre[b] and Oscar Lopez-Pamies *[a]

Received 9th September 2022,
Accepted 22nd November 2022

DOI: 10.1039/d2sm01219g

rsc.li/soft-matter-journal

A numerical and analytical study is made of the macroscopic or homogenized mechanical response of a random isotropic suspension of liquid n-spherical inclusions (n = 2, 3), each having identical initial radius A, in an elastomer subjected to small quasistatic deformations. Attention is restricted to the basic case when the elastomer is an isotropic incompressible linear elastic solid, the liquid making up the inclusions is an incompressible linear elastic fluid, and the interfaces separating the solid elastomer from the liquid inclusions feature a constant initial surface tension γ. For such a class of suspensions, it has been recently established that the homogenized mechanical response is that of a standard linear elastic solid and hence, for the specific type of isotropic incompressible suspension of interest here, one that can be characterized solely by an effective shear modulus $\overline{\mu}_n$ in terms of the shear modulus μ of the elastomer, the initial elasto-capillary number eCa = $\gamma/2\mu A$, the volume fraction c of inclusions, and the space dimension n. This paper presents numerical solutions—generated by means of a recently introduced finite-element scheme—for $\overline{\mu}_n$ over a wide range of elasto-capillary numbers eCa and volume fractions of inclusions c. Complementary to these, a formula is also introduced for $\overline{\mu}_n$ that is in quantitative agreement with all the numerical solutions, as well as with the asymptotic results for $\overline{\mu}_n$ in the limit of dilute volume fraction of inclusions ($c \searrow 0$) and at percolation ($c \nearrow p_n$). The proposed formula has the added theoretical merit of being an iterated-homogenization solution.

1 Introduction

Elastomers filled with liquid inclusions—contrary to conventional solid fillers—have emerged over the past few years as a new class of materials with unique macroscopic mechanical and physical properties.[1–5] From a qualitative point of view, the reasons for these unique properties are well settled. On one hand, as opposed to conventional solid fillers, the addition of liquid inclusions to elastomers increases the overall deformability and, on the other hand, the behavior of the interfaces separating a solid elastomer from embedded liquid inclusions, while negligible when the inclusions are "large", may dominate the macroscopic properties of the material when the inclusions are sufficiently "small". From a quantitative point of view, by contrast, the understanding of the fascinating properties of elastomers filled with liquid inclusions is yet to be fully developed.

In this context, Ghosh and Lopez-Pamies[6] and Ghosh, Lefèvre, and Lopez-Pamies[7] have recently worked out several theoretical results aimed at explaining and describing the mechanics of deformation of elastomers embedding liquid inclusions. They include the governing equations that describe the macroscopic or homogenized mechanical response of elastomers filled with liquid inclusions under finite quasistatic deformations, this for the fundamental non-dissipative case when:

- The elastomer is a hyperelastic solid,
- The liquid making up the inclusions is a hyperelastic fluid,
- The interfaces separating the solid elastomer from the liquid inclusions feature their own hyperelastic behavior, which includes the presence of an initial surface tension as a special case, and
- The inclusions are initially n-spherical‡ (n = 2, 3) in shape.

The equations show that the resulting macroscopic behavior of such filled elastomers is that of a hyperelastic solid—distinctly, one that depends directly on the size of the inclusions and the constitutive behavior of the interfaces—and hence that

[a] *Department of Civil and Environmental Engineering, University of Illinois, Urbana-Champaign, IL 61801, USA. E-mail: pamies@illinois.edu*
[b] *Department of Mechanical Engineering, Northwestern University, Evanston, IL 60208, USA*

† Electronic supplementary information (ESI) available. See DOI: https://doi.org/10.1039/d2sm01219g

‡ Following the terminology commonly employed by geometers,[8] we refer to circles as 2-spheres and to spheres as 3-spheres.

it is characterized by an effective stored-energy function $\overline{W}(\overline{\mathbf{F}})$ of the macroscopic deformation gradient $\overline{\mathbf{F}}$. What is more, the equations show that the effective stored-energy function $\overline{W}(\overline{\mathbf{F}})$ reduces asymptotically to the quadratic form

$$\overline{W}(\overline{\mathbf{F}}) = \frac{1}{2}\overline{\mathbf{H}} \cdot \overline{\mathbf{L}}\,\overline{\mathbf{H}} + O(\|\overline{\mathbf{H}}\|^3) \tag{1}$$

in the limit of small deformations as $\overline{\mathbf{H}} := \overline{\mathbf{F}} - \mathbf{I} \to 0$, where the initial effective modulus of elasticity

$$\overline{\mathbf{L}} := \frac{\partial^2 \overline{W}}{\partial \overline{\mathbf{F}} \partial \overline{\mathbf{F}}}(\mathbf{I}) \tag{2}$$

possesses the standard major and minor symmetries,

$$\overline{L}_{ijkl} = \overline{L}_{klij} \quad \text{and} \quad \overline{L}_{ijkl} = \overline{L}_{jikl} = \overline{L}_{ijlk}, \tag{3}$$

of a conventional linear elastic solid.

The result (1) is striking on two counts. First, the asymptotic behavior (1) implies that the macroscopic first Piola–Kirchhoff stress tensor specializes to

$$\overline{\mathbf{S}} = \frac{\partial \overline{W}}{\partial \overline{\mathbf{F}}}(\overline{\mathbf{F}}) = \overline{\mathbf{L}}\,\overline{\mathbf{H}} + O(\|\overline{\mathbf{H}}\|^2) \tag{4}$$

in the limit of small deformations as $\overline{\mathbf{H}} \to 0$ and hence that elastomers filled with liquid inclusions are free of macroscopic residual stresses (since $\overline{\mathbf{S}} = 0$ in the absence of deformation when $\overline{\mathbf{H}} = 0$), this in spite of the fact that there are local residual stresses within the underlying liquid inclusions due to the presence of initial interface stresses. Second, precisely because of the presence of local residual stresses within the liquid inclusions and of initial interface stresses, the local moduli of elasticity in the bulk and on the interfaces do not posses the standard minor symmetries of conventional elastic moduli. Yet, the resulting effective modulus of elasticity (2) turns out to possess the standard minor symmetries $(3)_2$. While the absence of a macroscopic residual stress in (4) is a direct consequence of the average of the local residual stresses within the inclusions canceling out the average of the initial interface stresses, the minor symmetries $(3)_2$ can be traced back to the effective stored-energy function (1) satisfying macroscopic material frame indifference.[6]

Granted the above general homogenization result, the object of this paper is to work out the solution for the effective modulus of elasticity $\overline{\mathbf{L}}$ for an isotropic incompressible elastomer filled with a random isotropic distribution of incompressible liquid n-spherical inclusions, each having identical (monodisperse) initial size, wherein the elastomer/liquid interfaces feature a constant initial surface tension. This, arguably, is the most basic type of elastomer filled with liquid inclusions. Clearly, by virtue of the symmetries (3), the effective modulus of elasticity for this type of isotropic incompressible filled elastomer is of the form

$$\overline{\mathbf{L}} = 2\overline{\mu}_n \mathbb{K} + \infty\, \mathbb{J}, \quad \begin{cases} \mathbb{K}_{ijkl} = \frac{1}{2}\left(\delta_{ik}\delta_{jl} + \delta_{il}\delta_{jk}\right) - \frac{1}{n}\delta_{ij}\delta_{kl} \\ \mathbb{J}_{ijkl} = \frac{1}{n}\delta_{ij}\delta_{kl} \end{cases}, \tag{5}$$

where $\mathbb{K}$ and $\mathbb{J}$ are the classical deviatoric and volumetric orthogonal projection tensors§ and where $\overline{\mu}_n$ stands for the effective shear modulus. The problem thus amounts to determining the effective shear modulus $\overline{\mu}_n$ in (5) directly in terms of the elasticity of the elastomer, the surface tension on the elastomer/liquid interfaces, and the size and amount of liquid inclusions.

We begin in Section 2 by formulating the homogenization problem that defines the pertinent effective modulus of elasticity (5). In Section 3, we discuss the asymptotic solutions for the effective shear modulus $\overline{\mu}_n$ in (5) in the limit of dilute volume fraction of inclusions and at percolation. The former is analytically tractable by means of plane/spherical harmonics. The latter, on the other hand, is analytically tractable only in part. In Section 4, we present numerical solutions—generated by means of a recently introduced finite-element scheme—for $\overline{\mu}_n$ over a wide range of volume fractions of inclusions between the dilute limit and percolation. Complementary to these numerical solutions, we then propose in Section 5 an explicit formula for $\overline{\mu}_n$. By construction, in direct analogy with a new result for suspensions of monodisperse rigid n-spheres,[9] the proposed formula is in quantitative agreement with all the asymptotic and numerical solutions presented in Sections 3 and 4 and, in addition, it has the theoretical merit of being an iterated-homogenization solution that is realizable by a certain class of random isotropic suspension of liquid n-spherical inclusions with infinitely many sizes. We devote Section 6 to describing the details of its realizability. We conclude in Section 7 by recording a few final comments.

At the close of this introduction, it is fitting to mention that several recent works,[10–13] motivated by the experiments of Style *et al.*,[2] have heuristically extended classical homogenization results in linear elasticity[14–16] to estimate an effective shear modulus $\overline{\mu}_3$ (and an effective bulk modulus $\overline{\kappa}_3$) for isotropic elastomers filled with isotropic distributions of incompressible liquid 3-spherical inclusions featuring a constant surface tension at the elastomer/liquid interfaces. In so doing, consciously or not, they have assumed that the presence of residual bulk and interface stresses and the lack of symmetry of the local moduli of elasticity do not change the type of homogenization limit. As summarized in the preceding paragraphs, the work of Ghosh and Lopez-Pamies[6] and Ghosh, Lefèvre, and Lopez-Pamies[7] has established that the type of homogenization limit, rather remarkably, does indeed remain of the classical form (1) with (3).

2 The problem

2.1 Initial configuration and kinematics

Consider a suspension comprised of a statistically uniform distribution of n-spherical inclusions, each having identical initial radius A, embedded in an elastomer that occupies a

§ Throughout, the components of all tensorial quantities are referred to a Cartesian frame of reference $\{\mathbf{e}_i\}$ (I = 1, …, n) and the summation convention is employed.

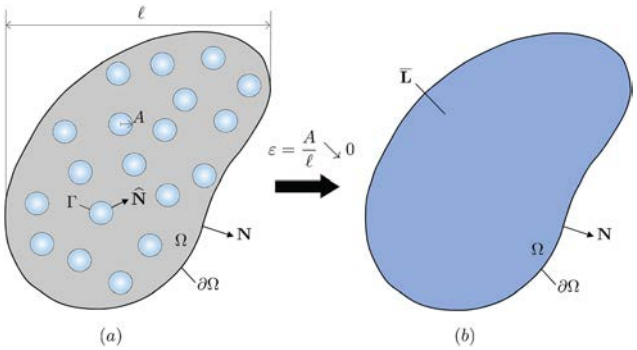

Fig. 1 (a) Schematic, in its initial undeformed configuration Ω, of a suspension of liquid n-spherical inclusions of monodisperse radius A embedded in an elastomer. (b) In the limit of separation of length scales as $\varepsilon = A/\ell \searrow 0$, when the inclusions are much smaller than the length scale ℓ of the domain Ω occupied by the body, the suspension can be shown[6,7] to behave as a homogeneous elastic solid. Specifically, within the setting of small quasistatic deformations, its mechanical response is fully characterized by an effective modulus of elasticity $\overline{\mathbf{L}}$.

domain $\Omega \subset \mathbb{R}^n$ ($n = 2, 3$) of length scale ℓ, with boundary $\partial\Omega$ and outward unit normal $\mathbf{N}$, in its initial undeformed configuration. Denote by Γ the smooth interfaces separating the inclusions from the elastomer, by $\hat{\mathbf{N}}$ the associated outward unit normal pointing from the inclusions towards the elastomer, and identify material points in the body by their initial position vector $\mathbf{X} \in \Omega$. See Fig. 1(a) for a schematic.

In response to a nominal traction $\bar{\mathbf{s}}(\mathbf{X})$ applied on the part of the boundary $\partial\Omega_{\mathcal{N}}$ and a displacement $\bar{\mathbf{u}}(\mathbf{X})$ applied on the complementary part of the boundary $\partial\Omega_{\mathcal{D}} = \partial\Omega \backslash \partial\Omega_{\mathcal{N}}$, the position vector $\mathbf{X}$ of a material point may occupy a new position $\mathbf{x}$ specified by a continuous¶ invertible mapping $\mathbf{x} = \mathbf{y}(\mathbf{X})$. In terms of the displacement field $\mathbf{u}(\mathbf{X}) := \mathbf{X} - \mathbf{y}(\mathbf{X})$, we write

$$\mathbf{x} = \mathbf{X} + \mathbf{u}(\mathbf{X}).$$

2.2 Constitutive behaviors of the bulk and the interfaces

All the inclusions are made of the same elastic fluid with first Lamé constant—or bulk modulus (since the shear modulus of an elastic fluid is zero)—$\Lambda_i > 0$ and have the same residual hydrostatic stress $r_i\mathbf{I}$. The elastomer, on the other hand, is an isotropic linear elastic solid with Lamé constants $\mu > 0$ and $\Lambda > 0$. As opposed to the inclusions, the elastomer is free of residual stresses. Moreover, the interfaces separating the elastomer from the inclusions exhibit a constant initial surface tension $\gamma \geq 0$.

Precisely, within the setting of small quasistatic deformations, the first Piola–Kirchhoff stress tensor $\mathbf{S}^\varepsilon$ at any material point in the bulk, $\mathbf{X} \in \Omega\backslash\Gamma$, reads[6]

$$\mathbf{S}^\varepsilon(\mathbf{X}) = r_i^\varepsilon(\mathbf{X})\mathbf{I} + \mathbf{L}^\varepsilon(\mathbf{X})\nabla\mathbf{u}^\varepsilon \tag{6}$$

with

$$\mathbf{L}^\varepsilon(\mathbf{X}) = r_i^\varepsilon(\mathbf{X})(\mathbb{A} - \mathbb{K} + (n-1)\mathbb{J}) + 2\mu^\varepsilon(\mathbf{X})\mathbb{K} + n\Lambda^\varepsilon(\mathbf{X})\mathbb{J}, \tag{7}$$

¶ We expect the interfaces between liquid inclusions and elastomers to be coherent, thus our restriction to continuous deformation fields.

where $\mathbb{A}_{ijkl} = 1/2(\delta_{ik}\delta_{jl} - \delta_{il}\delta_{jk})$ and where the superscript

$$\varepsilon := \frac{A}{\ell}$$

has been introduced to denote dependence on the size A of the inclusions and their spatial location. In particular, note that the dependence of the modulus of elasticity (7) on $\mathbf{X}$ is such that $r_i^\varepsilon(\mathbf{X}) = 0$, $\mu^\varepsilon(\mathbf{X}) = \mu$, $\Lambda^\varepsilon(\mathbf{X}) = \Lambda$ when $\mathbf{X}$ lies within the elastomer and $r_i^\varepsilon(\mathbf{X}) = r_i$, $\mu^\varepsilon(\mathbf{X}) = 0$, $\Lambda^\varepsilon(\mathbf{X}) = \Lambda_i$ when $\mathbf{X}$ lies within an inclusion.

Furthermore, the interface first Piola–Kirchhoff stress tensor $\hat{\mathbf{S}}^\varepsilon$ at any material point on the interfaces, $\mathbf{X} \in \Gamma$, reads[6]

$$\hat{\mathbf{S}}^\varepsilon(\mathbf{X}) = \gamma\hat{\mathbf{I}} + \hat{\mathbf{L}}\hat{\nabla}\mathbf{u}^\varepsilon \quad \text{with} \quad \hat{\mathbf{L}} = \gamma(\hat{\mathbb{A}} - \hat{\mathbb{K}} + \hat{\mathbb{J}}), \tag{8}$$

where $\hat{\mathbf{I}} = \mathbf{I} - \hat{\mathbf{N}} \otimes \hat{\mathbf{N}}$, $\hat{\mathbb{A}}_{ijkl} = \delta_{ik}\hat{I}_{jl} - 1/2\big(\hat{I}_{ik}\hat{I}_{jl} + \hat{I}_{il}\hat{I}_{jk}\big)$, $\hat{\mathbb{K}}_{ijkl} = 1/2\big(\hat{I}_{ik}\hat{I}_{jl} + \hat{I}_{il}\hat{I}_{jk} - \hat{I}_{ij}\hat{I}_{kl}\big)$, $\hat{\mathbb{J}}_{ijkl} = 1/2\hat{I}_{ij}\hat{I}_{kl}$ and $\hat{\nabla}\mathbf{u}^\varepsilon = \nabla\mathbf{u}^\varepsilon\hat{\mathbf{I}}$ stands for the interface gradient of the displacement field. That is, in indicial notation, $\big(\hat{\nabla}\mathbf{u}^\varepsilon\big)_{ij} = \hat{I}_{kj}\partial u_i^\varepsilon/\partial X_k$

2.3 Local governing equations

Absent inertia and body forces, substitution of the bulk and interface constitutive relations (6) and (8) in the balance of momenta yields the Lagrangian equations of equilibrium[6]

$$\begin{cases} \mathrm{Div}\big[r_i^\varepsilon(\mathbf{X})\mathbf{I} + \mathbf{L}^\varepsilon(\mathbf{X})\nabla\mathbf{u}^\varepsilon\big] = 0, & \mathbf{X} \in \Omega\backslash\Gamma \\ \widehat{\mathrm{Div}}\Big[\gamma\hat{\mathbf{I}} + \hat{\mathbf{L}}\hat{\nabla}\mathbf{u}^\varepsilon\Big] - \big[\big[r_i^\varepsilon(\mathbf{X})\mathbf{I} + \mathbf{L}^\varepsilon(\mathbf{X})\nabla\mathbf{u}^\varepsilon\big]\big]\hat{\mathbf{N}} = 0, & \mathbf{X} \in \Gamma \\ [\mathbf{L}^\varepsilon(\mathbf{X})\nabla\mathbf{u}^\varepsilon]\mathbf{N} = \bar{\mathbf{s}}(\mathbf{X}), & \mathbf{X} \in \partial\Omega_{\mathcal{N}} \\ \mathbf{u}^\varepsilon(\mathbf{X}) = \bar{\mathbf{u}}(\mathbf{X}), & \mathbf{X} \in \partial\Omega_{\mathcal{D}} \end{cases} \tag{9}$$

for the displacement field $\mathbf{u}^\varepsilon(\mathbf{X})$. In these equations, $[\![\cdot]\!]$ is the jump operator across the interfaces Γ based on the convention $[\![f(\mathbf{X})]\!] = f^{(\mathrm{i})}(\mathbf{X}) - f^{(\mathrm{e})}(\mathbf{X})$, where $f^{(\mathrm{i})}$ (resp. $f^{(\mathrm{e})}$) denotes the limit of any given function $f(\mathbf{X})$ when approaching Γ from within the inclusion (resp. elastomer), while $\widehat{\mathrm{Div}}$ stands for the interface divergence operator. That is, in indicial notation, $(\widehat{\mathrm{Div}}\,\mathbf{T})_i = \hat{I}_{kj}\partial T_{ij}/\partial X_k$ when applied to a second-order tensor $\mathbf{T}$.

In the initial configuration, prior to the application of the boundary conditions $\bar{\mathbf{s}}(\mathbf{X})$ and $\bar{\mathbf{u}}(\mathbf{X})$, the displacement field $\mathbf{u}^\varepsilon(\mathbf{X}) = 0$ and hence the equations of equilibrium (9) reduce to

$$\begin{cases} \nabla r_i^\varepsilon(\mathbf{X}) = \mathbf{0}, \ \mathbf{X} \in \Omega\backslash\Gamma \\ \gamma\widehat{\mathrm{Div}}\hat{\mathbf{I}} - r_i^\varepsilon(\mathbf{X})\hat{\mathbf{N}} = \mathbf{0}, \ \mathbf{X} \in \Gamma \end{cases}, \tag{10}$$

which can be viewed as the definition of the residual hydrostatic stress $r_i\mathbf{I}$ within the inclusions required to balance out the constant initial surface tension γ on the elastomer/liquid interfaces. Given that the inclusions are initially n-spherical, the solution of (10) yields the constant

$$r_i = -\frac{(n-1)\gamma}{A},$$

the same for all the inclusions. Granted this last relation, it is a simple matter to deduce that the Lagrangian equations of equilibrium (9) reduce to

$$\begin{cases} \mathrm{Div}[\mathbf{L}^{\varepsilon}(\mathbf{X})\nabla\mathbf{u}^{\varepsilon}] = 0, \quad \mathbf{X} \in \Omega\backslash\Gamma \\ \widehat{\mathrm{Div}}\left[\hat{\mathbf{L}}\hat{\nabla}\mathbf{u}^{\varepsilon}\right] - [\![\mathbf{L}^{\varepsilon}(\mathbf{X})\nabla\mathbf{u}^{\varepsilon}]\!]\hat{\mathbf{N}} = 0, \quad \mathbf{X} \in \Gamma \\ [\mathbf{L}^{\varepsilon}(\mathbf{X})\nabla\mathbf{u}^{\varepsilon}]\mathbf{N} = \bar{\mathbf{s}}(\mathbf{X}), \quad \mathbf{X} \in \partial\Omega_{\mathscr{N}} \\ \mathbf{u}^{\varepsilon}(\mathbf{X}) = \bar{\mathbf{u}}(\mathbf{X}), \quad \mathbf{X} \in \partial\Omega_{\mathscr{D}} \end{cases}. \tag{11}$$

2.4 Homogenization limit

In the limit of separation of length scales as $\varepsilon \searrow 0$, when the inclusions are much smaller than the length scale ℓ of the domain Ω occupied by the body, the solution $\mathbf{u}^{\varepsilon}(\mathbf{X})$ of the local equations of equilibrium (11) converges to a macroscopic displacement field $\mathbf{u}(\mathbf{X})$ solution of the homogenized equations of equilibrium[7]:

$$\begin{cases} \mathrm{Div}\left[\bar{\mathbf{L}}\nabla\mathbf{u}\right] = 0, \quad \mathbf{X} \in \Omega \\ [\bar{\mathbf{L}}\nabla\mathbf{u}]\mathbf{N} = \bar{\mathbf{s}}(\mathbf{X}), \quad \mathbf{X} \in \partial\Omega_{\mathscr{N}} \\ \mathbf{u}(\mathbf{X}) = \bar{\mathbf{u}}(\mathbf{X}), \quad \mathbf{X} \in \partial\Omega_{\mathscr{D}} \end{cases}. \tag{12}$$

In these equations, the constant fourth-order tensor $\overline{\mathbf{L}}$ is the effective modulus of elasticity that describes the macroscopic mechanical response of the suspension when subjected to small quasistatic deformations; see Fig. 1(b) for a schematic.

2.5 A formula for $\overline{\mathbf{L}}$

For the case of filled elastomers with periodic microstructure, much like for the classical case of linear elastic composite materials without residual and interface stresses,[17] the effective modulus of elasticity $\overline{\mathbf{L}}$ in (12) is expediently given by a formula that only involves computations over the unit cell defining the microstructure.

Precisely, taking the unit n-cube $\mathscr{Y} = (0,1)^n$ as the unit cell and denoting by

$$\theta(\mathbf{Y}) = \begin{cases} 1 & \text{if } \mathbf{Y} \text{ lies within an inclusion} \\ 0 & \text{else} \end{cases}$$

the $\mathscr{Y}$-periodic characteristic function that describes the initial spatial locations occupied by the inclusions, the formula for the effective modulus of elasticity—written here in a form that is valid for compressible as well as for nearly or completely incompressible constitutive behaviors for the elastomer and liquid inclusions—is given by[6,7]

$$\begin{aligned} \bar{L}_{ijkl} &= \int_{\mathscr{Y}} \left\{ L_{ijmn}(\mathbf{Y}) \left(\delta_{mk}\delta_{nl} + \frac{\partial \omega_{mkl}}{\partial Y_n}(\mathbf{Y}) \right) + \delta_{ij}\Sigma_{kl}(\mathbf{Y}) \right\} \mathrm{d}\mathbf{Y} \\ &\quad + \int_{\mathscr{Y}} \widehat{L}_{ijmn} \left(\delta_{mk}\widehat{I}_{nl} + \frac{\partial \omega_{mkl}}{\partial y_p}(\mathbf{Y}) \hat{I}_{pn} \right) \mathrm{d}\mathbf{Y}, \end{aligned} \tag{13}$$

where $\mathbf{L}(\mathbf{Y}) = (1-\theta(\mathbf{Y}))2\mu\mathbb{K} - \theta(\mathbf{Y})(n-1)\gamma/A(\mathbb{A} - \mathbb{K} + (n-1)\mathbb{J})$, $\mathscr{G}$ denotes the elastomer/liquid interfaces contained in $\mathscr{Y}$, the interface modulus of elasticity $\hat{\mathbf{L}}$ is given by $(8)_2$, and $\omega_{ijk}(\mathbf{Y})$ and $\Sigma_{ij}(\mathbf{Y})$ are the $\mathscr{Y}$-periodic functions defined as the solution of the unit-cell problem

$$\begin{cases} \dfrac{\partial}{\partial Y_j}\left[L_{ijkl}(\mathbf{Y}) \dfrac{\partial \omega_{kmn}}{\partial Y_l}(\mathbf{Y}) + \delta_{ij}\Sigma_{mn}(\mathbf{Y}) \right] = -\dfrac{\partial L_{ijmn}}{\partial Y_j}(\mathbf{Y}), \ \ \mathbf{Y} \in \mathscr{Y}\backslash\mathscr{G} \\ \dfrac{\partial}{\partial Y_q}\left[\hat{L}_{ijkl} \dfrac{\partial \omega_{kmn}}{\partial Y_p}(\mathbf{Y}) \hat{I}_{pl} \right] \hat{I}_{qj} - \left[\!\left[L_{ijkl}(\mathbf{Y}) \dfrac{\partial \omega_{kmn}}{\partial Y_l}(\mathbf{Y}) + \delta_{ij}\Sigma_{mn}(\mathbf{Y}) \right]\!\right] \hat{N}_j = \\ \quad -\dfrac{\partial}{\partial Y_q}\left[\hat{L}_{ijkl}\delta_{km}\hat{I}_{nl} \right] \hat{I}_{qj} + \left[\left[L_{ijkl}(\mathbf{Y})\delta_{km}\delta_{ln} + \delta_{ij}\Sigma_{mn}(\mathbf{Y}) \right] \right] \hat{N}_j, \ \ \mathbf{Y} \in \mathscr{G}. \\ \dfrac{\partial \omega_{imn}}{\partial Y_i}(\mathbf{Y}) - \dfrac{1}{n[(1-\theta(\mathbf{Y}))\Lambda + \theta(\mathbf{Y})\Lambda_i]}\Sigma_{mn}(\mathbf{Y}) = 0, \ \ \mathbf{Y} \in \mathscr{Y}\backslash\mathscr{G} \\ \int_{Y} \omega_{kmn}(\mathbf{Y})\mathrm{d}\mathbf{Y} = 0 \end{cases} \tag{14}$$

The computation of the effective modulus of elasticity $\overline{\mathbf{L}}$ for a given filled elastomer of interest amounts thus to solving the unit-cell problem (14) for the functions $\omega_{ijk}(\mathbf{Y})$ and $\Sigma_{ij}(\mathbf{Y})$ and then carrying out the integral in (13). In general, the unit-cell problem (14) can only be solved numerically.

Remark 1. While the unit-cell problem (14) can be solved directly for the components of the so-called concentration tensors ω_{ijk} and Σ_{ij} all at once, its linearity also allows to solve for the individual components of ω_{ijk} and Σ_{ij} one at a time. To see this, note that after multiplying (14) by a constant second-order tensor $\overline{H}_{\mathrm{mn}}$, $\omega_{\mathrm{kmn}}\overline{H}_{\mathrm{mn}}$ and $\Sigma_{\mathrm{mn}}\overline{H}_{\mathrm{mn}}$ are nothing more than the displacement field $u_k(\mathbf{Y})$ and pressure field $p(\mathbf{Y})$ in a unit-cell problem subjected to an average strain $\overline{H}_{\mathrm{mn}}$.

2.6 The specific case on interest here

The object of this paper is to determine the effective modulus of elasticity (13) for the basic case when the elastomer is incompressible

$$\Lambda = +\infty,$$

the liquid making up the inclusions is also incompressible

$$\Lambda_i = +\infty,$$

and the inclusions are randomly and isotropically distributed, this for any choice of shear modulus μ of the elastomer, any choice of initial surface tension γ, any choice of the initial size A of the inclusions, and any choice of volume fraction

$$c := \int_{\mathscr{Y}} \theta(\mathbf{Y})\mathrm{d}\mathbf{Y}$$

of inclusions from $c = 0$ to the percolation threshold $c = p_n$, where we recall that[18–20]

$$p_2 \approx 0.90 \quad \text{and} \quad p_3 \approx 0.64 \tag{15}$$

for 2- and 3-spherical inclusions, respectively.

Remark 2. As anticipated in the Introduction, because of the overall constitutive isotropy and incompressibility of the elastomer and the liquid making up the inclusions together with the overall geometric isotropy of the inclusions, the effective

modulus of elasticity (13) for the filled elastomer of interest here is of the isotropic incompressible form

$$\overline{\mathbb{L}} = 2\overline{\mu}_n \mathbb{K} + \infty \mathbb{J}.$$

Id est, the macroscopic response of the filled elastomer is fully characterized by an effective shear modulus $\overline{\mu}_n$. What is more, it follows from the definition (13) that $\overline{\mu}_n$ is of the functional form

$$\overline{\mu}_n = h(\mathrm{eCa}, c, n)\mu, \tag{16}$$

where eCa stands for the initial elasto-capillary number

$$\mathrm{eCa} := \frac{\gamma}{2\mu A}$$

and $h(\mathrm{eCa},c,n)$ is a function solely of its three indicated arguments.

Remark 3. In principle, to deal with a random and isotropic distribution of inclusions, one would have to consider unit cells $\mathscr{Y}$ that contain infinitively many inclusions. In practice, as elaborated in Section 4 below, away from percolation, it suffices to consider unit cells that contain a sufficiently large but finite number N of inclusions.[21–23] As one approaches percolation, however, that number N increases without bound.

3 Analytical solutions in the dilute limit and at percolation

In general, the solution of the unit-cell problem (14) needed to determine (13) is accessible only numerically. There are, however, two limiting cases in which (14) can be treated analytically or quasi-analytically and hence in which the effective shear modulus $\overline{\mu}_n$ can be determined in closed or quasi-closed form: (i) the limit of dilute volume fraction of inclusions when $c \searrow 0$ and (ii) the percolation limit when $c \nearrow p_n$. We discuss them next, one at a time.

3.1 The dilute limit

In the limit of dilute volume fraction of inclusions as $c \searrow 0$, it suffices to consider a unit cell $\mathscr{Y}$ that contains a single inclusion whose size relative to that of the unit cell is infinitesimally smaller. The asymptotic problem that results from (14)—that of a single inclusion embedded in an infinite medium—can then be solved analytically in terms of plane/spherical harmonics.[24] Making use of an Eulerian approach, Style *et al.*[10] worked out the solution in space dimension $n = 3$ and determined in turn the corresponding effective shear modulus $\overline{\mu}_3$. The same solution worked out within a Lagrangian setting can be found in Appendix D of Ghosh and Lopez-Pamies.[6] More generally, the solution for space dimension n is given by

$$\overline{\mu}_n = \mu + \frac{(2+n)(\mathrm{eCa}-1)}{n+(2+n)\mathrm{eCa}}\mu c + O(c^2). \tag{17}$$

In the absence of surface tension on the elastomer/liquid interfaces, when $\gamma = 0$ and hence $\mathrm{eCa} = 0$, the dilute solution (17) reduces identically to the classical Eshelby solution[14]

$$\overline{\mu}_n^{\mathrm{dil,liq}} = \mu - \left(1 + \frac{2}{n}\right)\mu c + O(c^2)$$

for the effective shear modulus of a dilute suspension of incompressible n-spherical inclusions of vanishingly small shear stiffness embedded in an isotropic incompressible solid. For later reference, we recall that for the more general case when the n-spherical inclusions are not liquid but just incompressible with shear modulus μ_i, the corresponding Eshelby solution reads

$$\overline{\mu}_n^{\mathrm{dil}} = \mu + \frac{(2+n)(\mu_i - \mu)}{n\mu + 2\mu_i}\mu c + O(c^2). \tag{18}$$

In the presence of surface tension, when $\gamma > 0$ and hence $\mathrm{eCa} > 0$, the dilute solution (17) is a monotonically increasing function of the elasto-capillary number eCa such that

$$\begin{cases} \overline{\mu}_n < \mu & \text{if } \mathrm{eCa} < 1 \\ \overline{\mu}_n = \mu & \text{if } \mathrm{eCa} = 1 \\ \overline{\mu}_n > \mu & \text{if } \mathrm{eCa} > 1 \end{cases}.$$

In other words, the presence of inclusions goes unnoticed at $\mathrm{eCa} = 1$ in the sense that the macroscopic response is identical to that of the elastomer without the inclusions. For $\mathrm{eCa} < 1$, the presence of inclusions leads to the softening of the macroscopic response relative to that of the elastomer, while it leads to its stiffening for $\mathrm{eCa} > 1$. This behavior stems from the fact that the presence of surface tension makes the inclusions resist deformation thereby providing a stiffening mechanism, one that increases with increasing elasto-capillary number eCa. For $\mathrm{eCa} > 1$, this stiffening mechanism is stronger than the softening provided by the lack of shear stiffness within the inclusions. In this regard, note that the dilute solution (17) reduces to

$$\overline{\mu}_n = \mu + \mu c + O(c^2) \tag{19}$$

in the limit as $\mathrm{eCa} \to +\infty$, when the inclusions pose the largest resistance to deformation and remain in fact n-spherical. Interestingly, as already noted by Taylor[25] for $n = 3$, this last result is different—in particular, softer—than the classical Einstein–Eshelby solution

$$\overline{\mu}_n^{\mathrm{dil,rig}} = \mu + \left(1 + \frac{n}{2}\right)\mu c + O(c^2)$$

for the effective shear modulus of a dilute suspension of rigid n-spherical inclusions embedded in an isotropic incompressible solid. The reason for this (factor of $1 + n/2$) difference is that the forces at a solid/liquid-inclusion interface featuring surface tension are different from those at a solid/rigid-inclusion interface, even in the limit as $\mathrm{eCa} \to +\infty$.

Remark 4. The computation of the correction of $O(c^2)$ in the Eshelby solution for n-spherical inclusions has been extensively studied,[26–30] the case of 3-spheres more so than that of 2-spheres. The techniques developed in those studies might

be applicable to the more general problem of interest in this work. Whether that is the case is worth exploring in future work. Here, for completeness, we simply recall the available correction[29] to $O(c^2)$ in (17) for $n = 3$ in the absence of surface tension on the interfaces, when $\gamma = 0$ and hence eCa = 0:

$$\overline{\mu}_3 = \mu - \frac{5}{3}\mu c + \frac{1}{2}\mu c^2 + O(c^3). \tag{20}$$

3.2 Percolation

It is well-known from experiments and computations[18–20] on the random packing of n-spheres that the maximum volume fraction c of n-spherical inclusions possible in the monodisperse filled elastomer of interest in this work is given by the percolation thresholds p_n spelled out in (15).

In the limit as $c \nearrow p_n$, contrary to the dilute limit discussed above, the isotropic distribution of the inclusions dictates that we have no option but to consider a unit cell $\mathscr{Y}$ that contains infinitely many inclusions; see Remark 3 above. This makes the asymptotic problem that results from (14) challenging. This traverse notwithstanding, it is still possible to determine analytical approximations for the effective shear modulus $\overline{\mu}_n$ as $c \nearrow p_n$,.

Space dimension $n = 2$. When the volume fraction c of n-spherical inclusions reaches the percolation threshold p_n, the inclusions come into direct contact with one another at several points. For space dimension $n = 2$—but not for space dimension $n = 3$—the number of points of contact (the so-called coordination number) is dense enough that the surrounding elastomer is fully severed into disconnected pieces. This implies that the elasticity of the elastomer plays no role in the governing equations at percolation; in other words, setting $\mu = 0$ would not change the response of the suspension. In turn, this implies that the surface tension γ can be factored out of the asymptotic problem stemming from (14) when $c = p_2$ and, in consequence, that the associated effective shear modulus that results from the definition (13) is necessarily of the simple asymptotic form

$$\lim_{c \nearrow p_2} \overline{\mu}_2 = \zeta_2 \frac{\gamma}{2A}, \tag{21}$$

where ζ_2 is a constant.

Now, the exact determination of the constant ζ_2 in (21) is a difficult endeavor because one has to deal with a unit cell $\mathscr{Y}$ that contains infinitely many inclusions. Nevertheless, it is possible to determine it approximately.

Princen[31] estimated that the effective shear modulus of a hexagonal—rather than random isotropic—distribution of monodisperse liquid 2-spherical inclusions at percolation, when $c = \pi/2\sqrt{3} \approx 0.9069$, is given by

$$\overline{\mu}_2^{\text{Hex,perc}} \approx 0.99 \frac{\gamma}{2A}. \tag{22}$$

It later emerged that the elastic response of a random isotropic suspension of 2-spheres at percolation is likely the same as that of a hexagonal suspension.[19,20] This is because both of these microstructures lead to a macroscopic elastic response that is isotropic, they have practically identical percolation thresholds, and, moreover, random isotropic suspensions contain clusterings of hexagonally packed inclusions. Motivated by these findings, as elaborated in Appendix A, we have determined numerically the effective shear modulus $\overline{\mu}_2^{\text{Hex}}$ of a hexagonal suspension of monodisperse liquid 2-spherical inclusions up to a volume fraction $c = 0.9050$.‖ By extrapolating the computed results to the percolation threshold $c = \pi/2\sqrt{3} \approx 0.9069$, we have then established that

$$\overline{\mu}_2^{\text{Hex,perc}} \approx 0.97 \frac{\gamma}{2A}, \tag{23}$$

which is not far from the estimate obtained by Princen.[31] Assuming that the response of a random isotropic suspension of monodisperse liquid 2-spherical inclusions at percolation is indeed essentially the same as that of the corresponding hexagonal suspension, for definiteness, we take

$$\zeta_2 = 1 \tag{24}$$

as the constant in the percolation limit (21) for space dimension $n = 2$.

Space dimension $n = 3$. For space dimension $n = 3$, contrary to $n = 2$, the number of points at which the inclusions come into contact at percolation when $c = p_3$ are *not* dense enough to severe the surrounding elastomer into disconnected pieces. In other words, the surrounding elastomer remains as a single piece of material, albeit one with communicating holes. Accordingly, the elasticity of the elastomer and not only the stiffness due to surface tension contribute to the effective shear modulus $\overline{\mu}_3$ of the suspension at percolation. In view of the general functional form (16), we have, in particular,

$$\lim_{c \nearrow p_3} \overline{\mu}_3 = \eta_3(\text{eCa})\mu, \tag{25}$$

where η_3(eCa) is a function solely of the elasto-capillary number.

For eCa $\gg$ 1, when the elasticity of the elastomer is negligible relative to the stiffness due to surface tension, it follows from (13) and (14) that

$$\eta_3(\text{eCa}) = \zeta_3 \text{eCa},$$

where ζ_3 is a constant. For arbitrary values of the elasto-capillary number eCa, however, the determination of the functional form of η_3(eCa) is difficult, again, because one has to deal with a unit cell $\mathscr{Y}$ that contains infinitely many inclusions. To gain insight, as elaborated in Appendix B, we have determined numerically the two effective (axisymmetric and simple) shear moduli, $\overline{\mu}_3^{\text{BCC}_a}$ and $\overline{\mu}_3^{\text{BCC}_s}$, of a body-centered cubic (BCC) suspension** of monodisperse liquid 3-spherical inclusions up to a volume fraction $c = 0.675$, which is very close to their

‖ Reaching such high values very near percolation is numerically challenging but doable because the pertinent unit cell contains a small number of inclusions, in our case, only two inclusions.

** For space dimension $n = 3$, in contrast to $n = 2$, there is no simple periodic suspension of monodisperse 3-spheres that leads to a macroscopic elastic response that is isotropic. As elaborated below, a BCC suspension can be thought of as the "next best thing".

percolation threshold $c = \sqrt{3}\pi/8 \approx 0.6802$. By extrapolating the computed results to the percolation threshold $c = \sqrt{3}\pi/8 \approx 0.6802$, we have then established that

$$\overline{\mu}_3^{\mathrm{BCC_a,perc}} \approx \frac{18}{1+0.00174\mathrm{eCa}^9} + \frac{1.69\left(104+\mathrm{eCa}-\frac{18}{1+0.00174\mathrm{eCa}^9}\right)\mathrm{eCa}}{0.79+\mathrm{eCa}} \tag{26}$$

and

$$\overline{\mu}_3^{\mathrm{BCC_s,perc}} \approx \frac{16}{1+0.00019\mathrm{eCa}^9} + \frac{0.48\left(405+\mathrm{eCa}-\frac{16}{1+0.00019\mathrm{eCa}^9}\right)\mathrm{eCa}}{0.95+\mathrm{eCa}}. \tag{27}$$

Now, while the macroscopic response of a BCC suspension is cubic and *not* isotropic, the results in Appendix B show that the extent of anisotropy for the case of liquid inclusions of interest here, as measured by the difference $\overline{\mu}_3^{\mathrm{BCC_a}} - \overline{\mu}_3^{\mathrm{BCC_s}}$, is not large. Moreover, the percolation threshold $c = \sqrt{3}\pi/8 \approx 0.6802$ and coordination number $z = 8$ of a BCC suspension are similar to the percolation threshold $p_3 \approx 0.64$ and average coordination number $\overline{z} \approx 6.5$ of a random isotropic suspension.[32] For these reasons, it is sensible to assume that the functional form of the function $\eta_3(\mathrm{eCa})$ in (25) is the same as that found for (26) and (27). We therefore posit that

$$\eta_3(\mathrm{eCa}) = \frac{a_3}{1+b_3\mathrm{eCa}^9} + \frac{(1+c_3)\left(1-\frac{a_3}{1+b_3\mathrm{eCa}^9}\right)+(\mathrm{eCa}-1)\zeta_3}{c_3+\mathrm{eCa}}\mathrm{eCa}$$

and hence that

$$\lim_{c\nearrow p_3}\overline{\mu}_3 = \frac{a_3\mu}{1+b_3\mathrm{eCa}^9} + \frac{(1+c_3)\left(1-\frac{a_3}{1+b_3\mathrm{eCa}^9}\right)+(\mathrm{eCa}-1)\zeta_3}{c_3+\mathrm{eCa}}\frac{\gamma}{2A}, \tag{28}$$

where, much like ζ_3, a_3, b_3, and c_3 are constants. The first describes the value of the effective shear modulus $\lim_{c\nearrow p_3}\overline{\mu}_3 = a_3\mu$ at eCa = 0, while the latter two modulate the transition from $a_3\mu$ to $\zeta_3\gamma/2A$ as eCa increases. The numerical results presented in the next section suggest that

$$a_3 = 0.1800, \quad b_3 = 0.0017, \quad c_3 = 0.7878, \quad \zeta_3 = 0.0169. \tag{29}$$

Remark 5. The apparent elasticity that foams and emulsions containing monodisperse 3-spherical inclusions exhibit at percolation has been the subject of many studies in the literature.[33–38] Such a behavior falls squarely within the formulation presented here when considering $\mathrm{eCa} \gg 1$, since for large elasto-capillary numbers the elasticity of the elastomer surrounding the liquid inclusions is negligible. The various existing approximations for foams and emulsions indicate that[34–38]

$$\lim_{c\nearrow p_3}\overline{\mu}_3 \approx (1.01\pm 0.09)\frac{\gamma}{2A}.$$

All such estimates overpredict the result $\lim_{c\nearrow p_3}\overline{\mu}_3 \approx 0.0169\frac{\gamma}{2A}$ suggested by our simulations for $\mathrm{eCa} \gg 1$.

A unifying expression for space dimension *n*. For space dimension n, in view of expressions (21) and (28), we can compactly write

$$\lim_{c\nearrow p_n}\overline{\mu}_n = \eta_n(\mathrm{eCa})\mu \tag{30}$$

with

$$\eta_n(\mathrm{eCa}) = \frac{a_n}{1+b_n\mathrm{eCa}^9} + \frac{(1+c_n)\left(1-\frac{a_n}{1+b_n\mathrm{eCa}^9}\right)+(\mathrm{eCa}-1)\zeta_n}{c_n+\mathrm{eCa}}\mathrm{eCa}, \tag{31}$$

where the values of the constants a_n, b_n, c_n, ζ_n are given in Table 1.

Table 1 Values of the constants in the function $\eta_n(\mathrm{eCa})$ for space dimensions n = 2 and 3

n	a_n	b_n	c_n	ζ_n
2	0	0	0	1
3	0.1800	0.0017	0.7878	0.0169

4 Numerical solutions for finite volume fraction of inclusions

In this section, we present numerical solutions for the effective shear modulus $\overline{\mu}_n$ over the range $\mathrm{eCa} \in [0,10]$ of elasto-capillary numbers and the ranges $c \in [0,0.6]$ and $c \in [0,0.5]$ of volume fractions of inclusions in space dimensions $n = 2$ and 3, respectively. Making use of a recently developed finite-element (FE) scheme,[6] the solutions are generated by solving numerically the unit-cell problem (14) over suitably selected unit cells $\mathscr{Y}$ and then computing the resulting effective modulus of elasticity (13).

4.1 Construction of the unit cells $\mathscr{Y}$

Prior to presenting the results themselves, we outline the procedure by which we constructed the unit cells $\mathscr{Y}$.

As noted in Remark 3 above, in order to model the type of *isotropic* filled elastomer of interest here, it suffices to consider unit cells containing random distributions of a finite number N of inclusions that is large enough that the resulting effective modulus of elasticity (13) is indeed isotropic to a high degree of accuracy. Here, we follow in the footstep of recent contributions[7,23] to construct the pertinent unit cells.

In a nutshell, we first constructed tens of thousands of realizations with the algorithm introduced by Lubachevsky and Stillinger[19] for unit cells $\mathscr{Y}$ containing up to 960 randomly distributed 2-spheres with volume fractions in the range $c \in [0,0.6]$ and randomly distributed 3-spheres with volume fractions in the range $c \in [0,0.5]$ for several fixed values of the minimum distance d between the n-spherical inclusions. We then filtered out the realizations that did not exhibit an isotropic elastic response to within a stringent tolerance. Precisely, realizations whose effective modulus of elasticity $\bar{\mathbf{L}}$ did not satisfy the condition

$$\frac{\left\|\mathbb{K}\bar{\mathbf{L}}\mathbb{K} - 2\overline{\mu}_n\mathbb{K}\right\|_\infty}{\left\|\mathbb{K}\bar{\mathbf{L}}\mathbb{K}\right\|_\infty} \leq 0.02 \quad \text{with} \quad \overline{\mu}_n := \frac{1}{n(1+n)-2}\mathbb{K}\cdot\bar{\mathbf{L}} \qquad (32)$$

were discarded as not sufficiently isotropic. This last relation, where we recall that $\mathbb{K}$ stands for the deviatoric orthogonal projection tensor $(5)_2$, serves to define the effective shear modulus $\overline{\mu}_n$ in terms of the entire effective modulus of elasticity (13) that is computed numerically.

The maximum difference in effective shear modulus $(32)_2$ between any two realizations (with the same elasto-capillary number eCa, volume fraction c, and minimum inter-inclusion distance d) that did satisfy condition $(32)_1$ was small, less than 2%. This confirmed that the values $(32)_2$ obtained for $\overline{\mu}_n$ could indeed be considered[39] as the effective shear modulus of an isotropic incompressible elastomer filled with a random isotropic suspension of liquid n-spherical inclusions of monodisperse size.

For completeness, we have included as ESI† two realizations that satisfy (32) for each of the volume fractions c = 0.1, 0.2, 0.3, 0.4, 0.5, 0.6 that we have considered in space dimension n = 2 and for each of the volume fractions c = 0.1, 0.2, 0.3, 0.4, 0.5 that we have considered in space dimension n = 3. All these realizations correspond to a minimum inter-inclusion distance of d = 0.01A. For illustration purposes, moreover, Fig. 2 shows four of these realizations, two for n = 2, the other two for n = 3, for volume fractions c = 0.3 and 0.5 of inclusions.

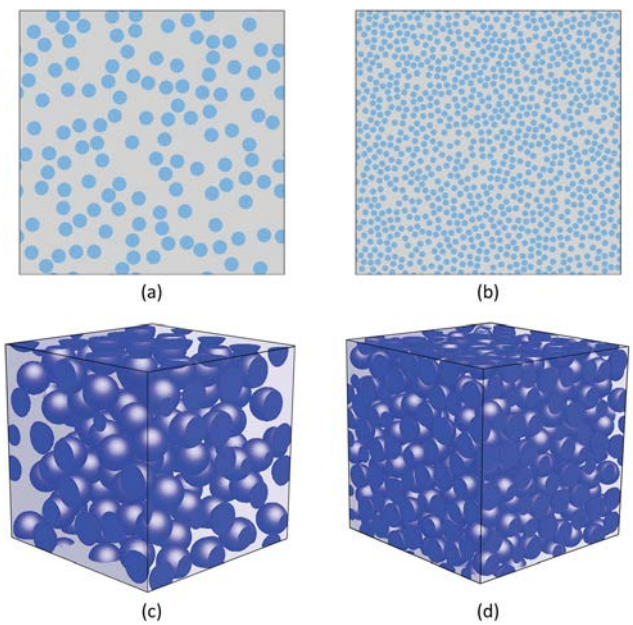

Fig. 2 Representative unit cells $\mathscr{Y}$ in space dimensions n = 2 and 3 containing random distributions of (a) N = 120 and (b) N = 960 2-spherical inclusions and (c) N = 120 and (d) N = 960 3-spherical inclusions of monodisperse radius A at volume fractions (a and c) c = 0.3 and (b and d) c = 0.5 and minimum distance d = 0.01A between the inclusions.

Remark 6. For definiteness, the FE results that we present throughout this work for $\overline{\mu}_n$ correspond to the average of all the realizations (with the same elasto-capillary number eCa, volume fraction c, and minimum inter-inclusion distance d) that satisfied condition (32). Moreover, for each elasto-capillary number eCa that we considered, the results are presented up to the maximum volume fraction c of inclusions for which we managed to generate converged solutions and correspond to the basic case of a vanishingly small minimum inter-inclusion distance, *i.e.*, d = 0+.

4.2 Results

Fig. 3 and 4 present the FE solutions (solid circles) obtained for the effective shear modulus $\overline{\mu}_n$ of a random isotropic suspension of monodisperse liquid n-spherical inclusions in an isotropic incompressible elastomer. While Fig. 3 shows the effective shear modulus $\overline{\mu}_2$ for 2-spherical inclusions, Fig. 4 shows the effective shear modulus $\overline{\mu}_3$ for 3-spherical inclusions. The results are presented normalized by the shear modulus μ of the elastomer as a function of the volume fraction c of inclusions for seven different values of elasto-capillary number, eCa = 0, 0.1, 0.5, 1, 2.5, 5, 10. For better quantitative visualization, parts (a) of the figures show the results for $0 \leq$ eCa < 1, while parts (b) show the results for eCa ≥ 1. For direct comparison, the figures also display the results based on the formula (33) introduced in the next section.

Three observations are immediate from Fig. 3 and 4. First, irrespectively of the volume fraction c of inclusions, the effective shear modulus $\overline{\mu}_n$ is a monotonically increasing function of the elasto-capillary number eCa. What is more, exactly as the behavior noted in the dilute limit,

$$\begin{cases} \overline{\mu}_n < \mu & \text{if eCa} < 1 \\ \overline{\mu}_n = \mu & \text{if eCa} = 1\,. \\ \overline{\mu}_n > \mu & \text{if eCa} > 1 \end{cases}$$

That is, while the presence of liquid inclusions leads to the softening of the macroscopic response relative to that of the elastomer when eCa < 1, it leads to its stiffening when eCa > 1. The transition from softening to stiffening still appears to occur at eCa = 1, at least up to the maximum volume fractions of inclusions that we considered. The explanation for this monotonic behavior in eCa remains the same as that for the dilute limit. Namely, the presence of surface tension (*i.e.*, eCa > 0) makes the inclusions resist deformation thereby providing a stiffening mechanism. For eCa > 1, this mechanism becomes strong enough that overtakes the softening provided by the lack of bulk shear stiffness within the inclusions resulting in the stiffening of the macroscopic response relative to that of the elastomer. The second immediate observation from Fig. 3 and 4 is that both the softening and the stiffening afforded by the presence of liquid n-spherical inclusions can be very

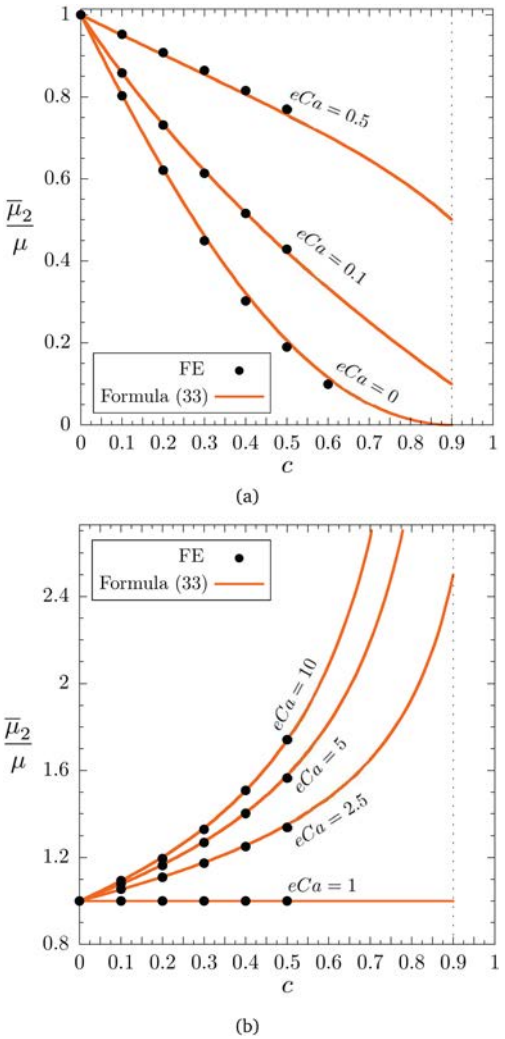

Fig. 3 Finite-element results (solid circles) for the effective shear modulus $\bar{\mu}_2$ of a random isotropic suspension of monodisperse liquid 2-spherical inclusions in an isotropic incompressible elastomer. The results are shown normalized by the shear modulus μ of the elastomer as a function of the volume fraction c of inclusions for elasto-capillary numbers $0 \leq \text{eCa} < 1$ in part (a) and for $\text{eCa} \geq 1$ in part (b). For direct comparison, the proposed formula (33) is also included (solid lines) in the figures.

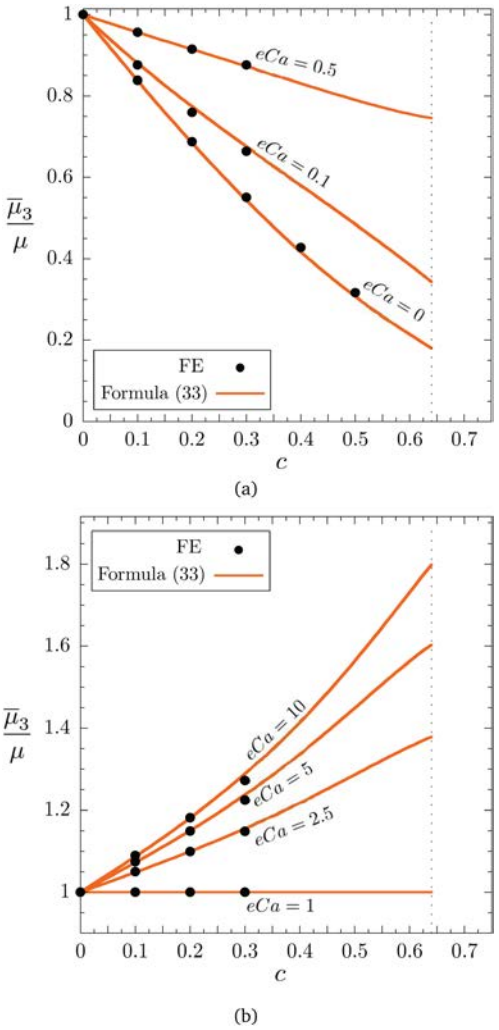

Fig. 4 Finite-element results (solid circles) for the effective shear modulus $\bar{\mu}_3$ of a random isotropic suspension of monodisperse liquid 3-spherical inclusions in an isotropic incompressible elastomer. The results are shown normalized by the shear modulus μ of the elastomer as a function of the volume fraction c of inclusions for elasto-capillary numbers $0 \leq \text{eCa} < 1$ in part (a) and for $\text{eCa} \geq 1$ in part (b). For direct comparison, the proposed formula (33) is also included (solid lines) in the figures.

significant even at moderate values of c and eCa. Finally, we note that the formula (33) is in good agreement with the FE solutions.

5 An explicit formula for $\overline{\mu}_n$

In this section, we show that the formula

$$\overline{\mu}_n = \mu\left[\left(1+\alpha_n(\text{eCa})\left(\frac{c}{p_n}\right)^2+\beta_n\left(\frac{c}{p_n}\right)^{n+1}\right)\left(1-\frac{c}{p_n}\right) + \left(\frac{c}{p_n}\right)^{3n-4}(\eta_n(\text{eCa}))^{-\frac{n+(2+n)\text{eCa}}{(2+n)p_n(\text{eCa}-1)}}\right]^{-\frac{(2+n)p_n(\text{eCa}-1)}{n+(2+n)\text{eCa}}}, \quad n=2,\,3, \tag{33}$$

with

$$\alpha_n(\text{eCa}) = \frac{d_n + f_n\text{eCa}}{e_n + g_n\text{eCa}}, \qquad \begin{cases}\beta_2 = 0\\ \\ \beta_3 = 0.4034\end{cases}, \tag{34}$$

where the values of the constants d_n, e_n, f_n, g_n are given in Table 2, and where we recall that p_n and $\eta_n(\text{eCa})$ are given by (15) and (31) for space dimensions $n = 2$ and 3, is in quantitative agreement with all the analytical results outlined in Section 3 and the numerical results presented in Section 4 and hence that it provides an accurate description for the effective shear modulus of a random isotropic suspension of monodisperse liquid n-spherical inclusions in an isotropic incompressible elastomer.

Table 2 Values of the constants in the function $\alpha_n(\mathrm{eCa})$ for space dimensions n = 2 and 3

n	d_n	e_n	f_n	g_n
2	−0.0002	0.0010	0.3634	1.7768
3	0.0016	0.0100	0.8170	1.2252

5.1 The dilute limit

In the limit as the volume fraction of inclusions $c \searrow 0+$, the effective shear modulus (33) reduces asymptotically to

$$\overline{\mu}_n = \mu + \frac{(2+n)(\mathrm{eCa}-1)}{n+(2+n)\mathrm{eCa}}\mu c + \frac{(2+n)(\mathrm{eCa}-1)}{2p_n}\left(\frac{1-2\alpha_n(\mathrm{eCa})}{n+(2+n)\mathrm{eCa}} - \frac{(3-n)(\eta_n(\mathrm{eCa}))^{-\frac{n+(2+n)\mathrm{eCa}}{(2+n)p_n(\mathrm{eCa}-1)}}}{1+2\mathrm{eCa}} + \frac{(2+n)p_n(\mathrm{eCa}-1)}{(n+(2+n)\mathrm{eCa})^2}\right) \times \mu c^2 + O(c^3). \tag{35}$$

Thus, irrespectively of the function $\alpha_n(\mathrm{eCa})$, constant β_n, and function $\eta_n(\mathrm{eCa})$, the formula (33) agrees identically with the exact dilute result (17).

5.2 Higher-order correction to the dilute limit for eCa = 0

For the case of 3-spherical inclusions and elasto-capillary number eCa = 0, the asymptotic result (35) specializes to

$$\overline{\mu}_3 = \mu - \frac{5}{3}\mu c + 0.5\mu c^2 + O(c^3).$$

This result agrees identically with the higher-order exact result (20).

5.3 Percolation

In the limit as the volume fraction of inclusions $c \nearrow p_n$, the effective shear modulus (33) reduces asymptotically to

$$\overline{\mu}_n = \eta_n(\mathrm{eCa})\mu + O(p_n - c). \tag{36}$$

Thus, the formula (33) also agrees identically with the corresponding result (30) at percolation.

5.4 Comparison with numerical solutions

For intermediate values of volume fraction c of inclusions away from the dilute limit and percolation, Fig. 3 and 4 above show comparisons between the formula (33) and the numerical solutions presented in Section 4. It is plain that both sets of results are in good quantitative agreement for all elasto-capillary numbers eCa and volume fractions c for which the numerical results are available.

5.5 The special cases of eCa = 0, 1, and + ∞

In the absence of surface tension on the elastomer/liquid interfaces, when eCa = 0, the effective shear modulus (33) reduces to

$$\overline{\mu}_n = \mu\left[\left(1 + \frac{d_n}{e_n}\left(\frac{c}{p_n}\right)^2 + \beta_n\left(\frac{c}{p_n}\right)^{n+1}\right)\left(1-\frac{c}{p_n}\right) + \left(\frac{c}{p_n}\right)^{3n-4} a_n^{\frac{n}{(2+n)p_n}}\right]^{\frac{(2+n)p_n}{n}}.$$

Moreover, for elasto-capillary number eCa = 1, the effective shear modulus (33) specializes to

$$\overline{\mu}_n = \mu = \frac{\gamma}{2A}.$$

That is, the presence of liquid inclusions goes unnoticed in the sense that $\overline{\mu}_n = \mu$ for any value of the volume fraction c of inclusions. Finally, for unbounded elasto-capillary number when eCa = $+\infty$, the effective shear modulus (33) reduces to

$$\overline{\mu}_n = \mu\left[\left(1 + \frac{f_n}{g_n}\left(\frac{c}{p_n}\right)^2 + \beta_n\left(\frac{c}{p_n}\right)^{n+1}\right)\left(1-\frac{c}{p_n}\right)\right]^{-p_n}.$$

As expected, in spite of the fact that the underlying inclusions do not deform and remain n-spherical when eCa = $+\infty$, this last result is significantly softer than the corresponding result for a suspension of monodisperse rigid n-spherical inclusions:[9]

$$\overline{\mu}_n^{\mathrm{rig}} = \mu\left[\left(1 + a_n\left(\frac{c}{p_n}\right)^2 + b_n\left(\frac{c}{p_n}\right)^{n+1}\right)\left(1-\frac{c}{p_n}\right)\right]^{-\frac{(2+n)p_n}{2}}, \tag{37}$$

where $a_2 = -0.238$, $b_2 = -0.299$, $a_3 = 0.017$, $b_3 = 0.635$ for space dimensions n = 2 and 3. The reason for this difference is the same already noted for the dilute result (19), namely, that the forces at a solid/liquid-inclusion interface featuring surface tension are different from those at a solid/rigid-inclusion interface, even for unbounded elasto-capillary number eCa = $+\infty$.

5.6 Connection with the classical differential scheme

The formula (33) can be thought of as a generalization of the classical differential-scheme (DS) result[40,41]

$$\overline{\mu}_{\mathrm{DS}_n}^{\mathrm{liq}} = \frac{\mu}{(1-c)^{-\frac{2+n}{n}}} \tag{38}$$

for the effective shear modulus of an isotropic suspension of polydisperse liquid n-spherical inclusions in an isotropic incompressible solid in that: (i) the volume fraction c is re-scaled†† by the percolation threshold $c \mapsto c/p_n$ and (ii) the stiffness due to the presence of a surface tension on the solid/liquid-inclusion interfaces is account for, including at percolation.

†† A re-scaling of this type, which can be traced back to the work of Eilers,[42] has been repeatedly used—albeit heuristically, disconnected from the differential scheme[40,41]—to model percolation in the analogous problem of the determination of the viscosity of suspensions of rigid 3-spheres in a Newtonian fluid.[43,44]

5.7 Realizability

In direct analogy with the effective shear modulus (37) for suspensions of monodisperse rigid n-spheres, the proposed formula (33) is not "just" a formula that happens to be in agreement with the above-summarized analytical and numerical results, but has also the merit to be realizable as an iterated-homogenization solution. Precisely, as elaborated in the next section, the formula (33) can be shown to be the exact homogenization solution for the effective shear modulus of a certain class of random isotropic suspensions of liquid n-spherical inclusions with infinitely many sizes in an isotropic incompressible elastomer. That the effective shear modulus (33) is descriptive of both isotropic suspensions with monodisperse and with (a specially selected class of) polydisperse liquid n-spherical inclusions is nothing more than a manifestation of the richness in behaviors that suspensions of polydisperse liquid n-spherical can exhibit.

6 Realizability

To show that the effective shear modulus (33) is realizable, we begin by extending the generalized differential scheme for linear elastostatics[45,46] to account for the presence of surface tension in the filled elastomer of interest here. The derivation goes as follows.

Consider the domain Ω to be initially occupied by a "backbone" elastomer, which we label $s = 0$ and take to be homogeneous, isotropic, and incompressible with, as of yet, arbitrary shear modulus $\mu^{(0)}$. Embed a dilute distribution of two different materials, labeled $s = 1$ and 2, one being n-spherical inclusions‡‡ made of another isotropic incompressible elastomer with shear modulus $\mu^{(1)}$, the other being n-spherical inclusions of monodisperse radius $A^{[1]}$ made of an incompressible liquid featuring an initial surface tension $\gamma^{[1]}$ at the interfaces with the "backbone" elastomer. Denoting the infinitesimal volume fractions of these two types of added materials by $v_1^{[1]}$ and $v_2^{[1]}$, respectively, it follows from use of the dilute solutions (18) and (17) that the resulting three-phase filled elastomer has an effective shear modulus $\widetilde{\mu}_n^{[1]}$ given by

$$\widetilde{\mu}_n^{[1]} = \mu^{(0)} + \frac{(2+n)(\mu^{(1)} - \mu^{(0)})}{n\mu^{(0)} + 2\mu^{(1)}}\mu^{(0)} v_1^{[1]} + \frac{(2+n)(\mathrm{eCa}^{[1]} - 1)}{n + (2+n)\mathrm{eCa}^{[1]}}\mu^{(0)} v_2^{[1]} \tag{39}$$

to order $O(1)$ in $v_1^{[1]}$ and $v_2^{[1]}$, where $\mathrm{eCa}^{[1]} = \gamma^{[1]}/2\mu^{(0)}A^{[1]}$.

Taking next the filled elastomer with shear modulus $\widetilde{\mu}_n^{[1]}$—rather than $\mu^{(0)}$—as the "backbone" elastomer, we repeat exactly the same addition of the two types of n-spherical inclusions in dilute proportions. This second iteration requires utilizing the same dilute distribution as in the first iteration, but with a larger length scale, since (39) is being employed as the shear modulus of a "homogenous" material. Denoting by $v_1^{[2]}$ and $v_2^{[2]}$ the infinitesimal volume fractions of materials $s = 1$ and 2 embedded in this second step, the resulting filled elastomer has now an effective shear modulus given by

$$\widetilde{\mu}_n^{[2]} = \widetilde{\mu}_n^{[1]} + \frac{(2+n)(\mu^{(1)} - \widetilde{\mu}_n^{[1]})}{n\widetilde{\mu}_n^{[1]} + 2\mu^{(1)}}\widetilde{\mu}_n^{[1]} v_1^{[2]} + \frac{(2+n)(\mathrm{eCa}^{[2]} - 1)}{n + (2+n)\mathrm{eCa}^{[2]}}\widetilde{\mu}_n^{[1]} v_2^{[2]}$$

with $\mathrm{eCa}^{[2]} = \gamma^{[2]}/2\overline{\mu}_n^{[1]}A^{[2]}$, where $\gamma^{[2]}$ and $A^{[2]}$ denote, respectively, the surface tension of the liquid at the interfaces with the new "backbone" material and the radius of the liquid inclusions. Note that we are at liberty to choose an arbitrary value for the ratio $\gamma^{[2]}/A^{[2]}$. Thus, we are at liberty to choose an arbitrary elasto-capillary number $\mathrm{eCa}^{[2]}$. Note further that the total volume fractions of materials $s = 1$ and 2 at this stage are given, respectively, by $\phi_1^{[2]} = v_1^{[2]} + \phi_1^{[1]}(1 - v_1^{[2]} - v_2^{[2]})$ and $\phi_2^{[2]} = v_2^{[2]} + \phi_2^{[1]}(1 - v_1^{[2]} - v_2^{[2]})$, where $\phi_1^{[1]} = v_1^{[1]}$ and $\phi_2^{[1]} = v_2^{[1]}$.

It is apparent now that repeating the same above process $k + 1$ times, for arbitrarily large $k \in \mathbb{N}$, generates a filled elastomer with effective shear modulus

$$\begin{aligned}\widetilde{\mu}_n^{[k+1]} &= \widetilde{\mu}_n^{[k]} + \frac{(2+n)(\mu^{(1)} - \widetilde{\mu}_n^{[k]})}{n\widetilde{\mu}_n^{[k]} + 2\mu^{(1)}}\widetilde{\mu}_n^{[k]} v_1^{[k+1]} \\ &\quad + \frac{(2+n)(\mathrm{eCa}^{[k+1]} - 1)}{n + (2+n)\mathrm{eCa}^{[k+1]}}\widetilde{\mu}_n^{[k]} v_2^{[k+1]},\end{aligned} \tag{40}$$

which contains total volume fractions of materials $s = 1$ and 2 given by

$$\begin{cases}\phi_1^{[k+1]} = v_1^{[k+1]} + \phi_1^{[k]}\left(1 - v_1^{[k+1]} - v_2^{[k+1]}\right) \\ \phi_2^{[k+1]} = v_2^{[k+1]} + \phi_2^{[k]}\left(1 - v_1^{[k+1]} - v_2^{[k+1]}\right)\end{cases}. \tag{41}$$

Fig. 5 provides a schematic illustration of the construction process leading to (40).

Upon inverting relations (41) in favor of $v_1^{[k+1]}$ and $v_2^{[k+1]}$, taking the limit of infinitely many iterations ($k \to \infty$), parameterizing the construction process with a time-like variable $t \in [0,1]$, and choosing $\mu^{(0)} = \mu^{(1)} = \mu$, the difference eqn (40) yields the first-order nonlinear ordinary differential equation (ODE)

$$\begin{aligned}(1 - \phi_1(t) - \phi_2(t))\frac{\mathrm{d}\widetilde{\mu}_n}{\mathrm{d}t}(t) &= \left[(1 - \phi_2(t))\frac{\mathrm{d}\phi_1}{\mathrm{d}t}(t) + \phi_1(t) \times \frac{\mathrm{d}\phi_2}{\mathrm{d}t}(t)\right] \\ &\quad \times \frac{(2+n)(\mu - \widetilde{\mu}_n(t))}{n\widetilde{\mu}_n(t) + 2\mu}\widetilde{\mu}_n(t) \\ &\quad + \left[(1 - \phi_1(t))\frac{\mathrm{d}\phi_2}{\mathrm{d}t}(t) + \phi_2(t)\frac{\mathrm{d}\phi_1}{\mathrm{d}t}(t)\right] \\ &\quad \times \frac{(2+n)(\widetilde{\mathrm{eCa}}(t) - 1)}{n + (2+n)\widetilde{\mathrm{eCa}}(t)}\widetilde{\mu}_n(t) \quad t \in (0,1],\end{aligned} \tag{42}$$

with initial condition

$$\widetilde{\mu}_n(0) = \mu, \tag{43}$$

that defines the effective shear modulus

$$\overline{\mu}_n = \widetilde{\mu}_n(1) \tag{44}$$

‡‡ For our purposes here, we consider that the material $s = 3$ is added in the form of n-spherical inclusions, but any other shape could be considered as well, so long as the amount of added material in infinitesimal.

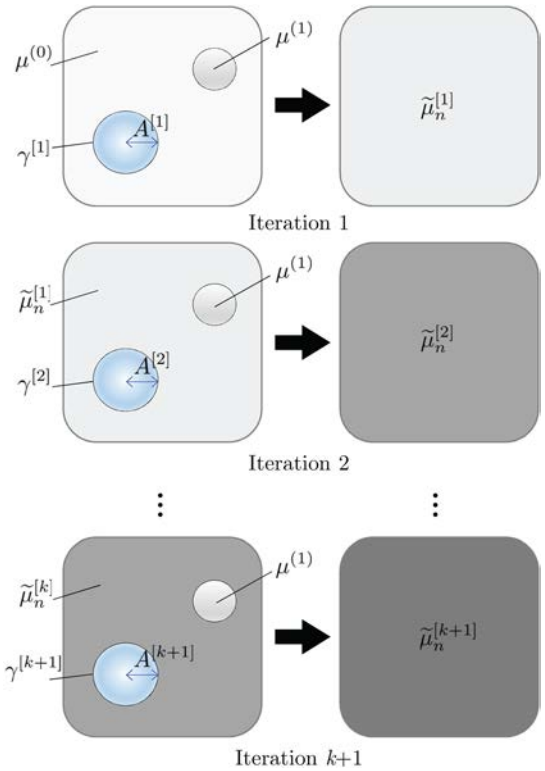

Fig. 5 Schematic of the of iterative construction process.

of a very large family of random isotropic suspensions of incompressible liquid n-spherical inclusions of infinitely many sizes in an incompressible isotropic elastomer with shear modulus μ.

In eqn (42), $\phi_1(t)$, $\phi_2(t)$, $\widetilde{\mathrm{eCa}}(t)$ stand for non-negative continuous functions of choice. The first two are subject to the inequality constraint $\phi_1(t) + \phi_2(t) \leq 1$. In addition, they must be selected so that the combinations $\phi_1(t)/(1 - \phi_1(t) - \phi_2(t))$ and $\phi_2(t)/(1 - \phi_1(t) - \phi_2(t))$ are monotonically increasing functions of t, $\phi_1(0) = \phi_2(0) = 0$, and $\phi_2(1) = c$. The specific choice of functions $\phi_1(t)$, $\phi_2(t)$, $\widetilde{\mathrm{eCa}}(t)$ defines the type of suspension being considered, that is, the specific sizes and spatial distributions of the liquid n-spherical inclusions as well as the specific elasto-capillary numbers at all length scales. Different choices of $\phi_1(t)$, $\phi_2(t)$, $\widetilde{\mathrm{eCa}}(t)$ lead hence to different solutions for the effective shear modulus $\overline{\mu}_n$ of the resulting suspension.

From a computational point of view, we remark that the ODE (42) needs to be solved from the initial condition (43) at $t = 0$ up to $t = 1$, as its solution then $\widetilde{\mu}_n(1)$ defines the effective shear modulus (44) of the suspension.

6.1 One-sided radial paths with constant path-independent elasto-capillary number

At this stage, it is a simple matter to deduce that the simple choice

$$\phi_1(t) = 0, \quad \phi_2(t) = ct, \quad \widetilde{\mathrm{eCa}}(t) = 0 \tag{45}$$

in the initial-value problem (42)–(44) leads to the classical *DS* result (38). The more general choice

$$\phi_1(t) = 0, \quad \phi_2(t) = ct, \quad \widetilde{\mathrm{eCa}}(t) = \mathrm{eCa}, \tag{46}$$

which accounts for the presence of surface tension *via* an elasto-capillary number $\widetilde{\mathrm{eCa}}(t)$ that is constant and the same for all length scales in the construction process, leads to the effective shear modulus

$$\overline{\mu}_{\mathrm{DS}_n} = \frac{\mu}{(1-c)^{\frac{(2+n)(\mathrm{eCa}-1)}{n+(2+n)\mathrm{eCa}}}}. \tag{47}$$

This result was recently introduced (for $n = 3$) by Ghosh and Lopez-Pamies[6] as the simplest differential-scheme result that accounts for surface tension.

Note that the construction paths (45) and (46) are one-sided and radial in the sense that only material $s = 2$ (*i.e.*, the liquid n-spherical inclusions) is added linearly in time t throughout the entire construction process. As a result, they lead to suspensions wherein the liquid n-spherical inclusions are spatially distributed in ways in which they can occupy the entire volume of the suspension at hand. For that reason, the ensuing effective shear moduli (38) and (47) percolate at $c = 1$.

6.2 General radial paths with constant path-dependent elasto-capillary number

To show that the result (33) proposed in this work is a solution of the initial-value problem (42)–(43), we need to consider the more general family of radial construction paths with constant but path-dependent elasto-capillary number

$$\phi_1(t) = \Phi_n(c)t, \quad \phi_2(t) = ct, \quad \widetilde{\mathrm{eCa}}(t) = \chi_n(c)\mathrm{eCa}, \tag{48}$$

where the functions $\Phi_n(c)$ and $\chi_n(c)$ satisfy the inequalities $0 \leq \Phi_n(c) \leq 1 - c$ and $\chi_n(c) \geq 0$ but are arbitrary otherwise. We emphasize that in the construction process (48)—contrary to (45) and (46)—material $s = 1$ (*i.e.*, the elastomer) and material $s = 2$ (*i.e.*, the liquid n-spherical inclusions) are both added linearly in time t, while the elasto-capillary number $\widetilde{\mathrm{eCa}}(t)$ is constant and the same for all length scales but its value $\chi_n(c)\mathrm{eCa}$ depends on the construction path *via* the final volume fraction c of liquid n-spherical inclusions.

Granted the family of construction paths (48), the initial-value problem (42)–(43) can be integrated into the closed form

$$\mathscr{E}(\overline{\mu}_n) = \left(\frac{2}{2+n} + \frac{\Phi_n}{cK} + \left(\frac{n}{2+n} - \frac{\Phi_n}{cK}\right)\frac{\overline{\mu}_n}{\mu}\right)^{\frac{\Phi_n(\Phi_n+c)(2+n)^2}{(2cK+(2+n)\Phi_n)((2+n)\Phi_n-cnK)}} - (1-\Phi_n-c)\left(\frac{\overline{\mu}_n}{\mu}\right)^{\frac{2(\Phi_n+c)}{2cK+(2+n)\Phi_n}} = 0, \tag{49}$$

where, for simplicity, we have introduced the notation $K = (2 + n)(\chi_n\mathrm{eCa} - 1)/(n + (2 + n)\chi_n\mathrm{eCa})$ and have omitted the argument c in Φ_n and χ_n. For a given choice of functions $\Phi_n(c)$ and $\chi_n(c)$, a given volume fraction c of liquid n-spherical inclusions, a given elasto-capillary number eCa, and a given

space dimension n, the nonlinear algebraic eqn (49) defines the effective shear modulus $\overline{\mu}_n$, normalized by the shear modulus μ of the underlying elastomer, of the resulting suspension.

For each of the elasto-capillary numbers eCa = 0, 0.1, 0.5, 1, 2.5, 5, 10 considered in the previous section, it is not difficult to show—*via* numerical solutions of (49)—that one can find a plurality of functions $\Phi_n(c)$ and $\chi_n(c)$ that do indeed lead to the effective shear modulus (33) thereby demonstrating that the proposed formula (33) is realizable by a suspension of liquid n-spherical inclusions with infinitely many sizes. Again, the fact that the effective shear modulus (33) is descriptive of both isotropic suspensions with monodisperse and with (a specially selected class of) polydisperse liquid n-spherical inclusions is nothing more than a manifestation of the wide range of behaviors that suspensions of polydisperse liquid n-spherical inclusions can exhibit.

7 Final comments

7.1 Suspensions with polydisperse 3-spherical inclusions with constant elasto-capillary number

It is instructive to compare the effective shear modulus (33) for isotropic suspensions of monodisperse 3-spherical inclusions with earlier results for suspensions of 3-spherical inclusions of infinitely many sizes featuring a constant elasto-capillary number. Those are the DS result[6] (47) already referenced above and the differential-coated-sphere (DCS) result worked out by Mancarella *et al.*[11] following in the footstep of Christensen and Lo.[16] The latter reads

$$\overline{\mu}_{\mathrm{DCS}_3} = \mu + \frac{70(\mathrm{eCa}-1)c}{21+35\mathrm{eCa}+30(1-\mathrm{eCa})c+(19-40\mathrm{eCa})c^{10/3}+\sqrt{q_3}}\mu \tag{50}$$

with

$$\begin{aligned} q_3 &= 49(3+5\mathrm{eCa})^2 - 28(1-\mathrm{eCa})(3+5\mathrm{eCa})c - 4700(1-\mathrm{eCa})^2c^2 \\ &\quad + 9408(1-\mathrm{eCa})c^{8/3} - 14(393-25(1+8\mathrm{eCa})\mathrm{eCa})c^{10/3} \\ &\quad + 4(1-\mathrm{eCa})(19-40\mathrm{eCa})c^{13/3} + (19-40\mathrm{eCa})^2c^{20/3}. \end{aligned}$$

In the limit of dilute volume fraction of 3-spherical inclusions as $c \searrow 0$, the effective shear moduli (47) and (50) reduce asymptotically to

$$\overline{\mu}_{\mathrm{DS}_3} = \mu + \frac{5(\mathrm{eCa}-1)}{3+5\mathrm{eCa}}\mu c + \frac{5(\mathrm{eCa}-1)(5\mathrm{eCa}-1)}{(3+5\mathrm{eCa})^2}\mu c^2 + O(c^3)$$

and

$$\overline{\mu}_{\mathrm{DCS}_3} = \mu + \frac{5(\mathrm{eCa}-1)}{3+5\mathrm{eCa}}\mu c + \frac{10(\mathrm{eCa}-1)^2}{(3+5\mathrm{eCa})^2}\mu c^2 + O(c^3). \tag{51}$$

As expected, the coefficients of $O(c^2)$ in both of these expressions are different from the one in (35). For eCa > 0 (but not for eCa = 0), a quantitative comparison reveals that the coefficient of $O(c^2)$ in (51) is closest to the one in (35). In this regard, it is also worth noting that the DCS result (50) happens to coincide identically up to and including $O(c^2)$ with the Hashin–Shtrikman (HS) formula

$$\overline{\mu}_{\mathrm{HS}_3} = \mu + \frac{5(\mathrm{eCa}-1)c}{3+2c+(5-2c)\mathrm{eCa}}\mu = \mu + 5\mu\sum_{k=1}^{\infty}\frac{2^{k-1}(\mathrm{eCa}-1)^k}{(3+5\mathrm{eCa})^k}c^k, \tag{52}$$

which was heuristically introduced[12] by replacing the shear modulus of one of the phases, say μ_i, in one of the HS bounds[15] for two-phase isotropic composite materials with an equivalent elasto-capillary stiffness, namely, $\mu_i = 8\mathrm{eCa}\mu/(5+3\mathrm{eCa})$. As opposed to (47) and (50), the HS formula (52) is not the homogenization solution of a suspension of 3-spherical inclusions.

The behaviors as $c \nearrow p_3$ of the effective moduli (47) and (50) are also very different from that (36) of formula (33). This is not surprising since the effective moduli (47) and (50) correspond to suspensions wherein the 3-spherical inclusions are of infinitely many different sizes and spatially distributed in ways in which they can occupy the entire volume of the suspension at hand, that is, they correspond to suspensions that percolate at $c = 1$, as opposed to at $c = p_3$.

7.2 Finite deformations

When considering finite quasistatic deformations, the homogenized behavior of a standard (without residual stresses and interfacial forces) hyperelastic composite material is characterized by an effective stored-energy function $\overline{W}(\overline{\mathbf{F}})$ that, in general, is functionally very different from the stored-energy functions that describe the underlying hyperelastic constituents. This is so even in the most specialized case of isotropic incompressible composite materials made of isotropic incompressible constituents, when the resulting effective stored-energy function $\overline{W}(\overline{\mathbf{F}})$, much like the local stored-energy function $W(\mathbf{X},\mathbf{F})$, admits representations in terms of just $n-1$ invariants.

Based on a wide range of analytical and numerical results that have appeared over the past two decades, as well as some new results, Lefèvre *et al.*[23] have recently conjectured that the case of isotropic incompressible Neo-Hookean elastomers in space dimension $n = 2$ is a rare exception to the aforementioned general rule. Precisely, these authors have posited that the homogenized behavior of an isotropic hyperelastic material comprised of incompressible Neo-Hookean elastomers with stored-energy function

$$W(\mathbf{X},\mathbf{F}) = \begin{cases} \dfrac{\mu(\mathbf{X})}{2}[\mathbf{F}\cdot\mathbf{F}-2] & \text{if } \det\mathbf{F}=1 \\ +\infty & \text{else} \end{cases}$$

is itself exactly Neo-Hookean with effective stored-energy function

$$\overline{W}(\overline{\mathbf{F}}) = \begin{cases} \dfrac{\overline{\mu}}{2}[\overline{\mathbf{F}}\cdot\overline{\mathbf{F}}-2] & \text{if } \det\overline{\mathbf{F}}=1 \\ +\infty & \text{else} \end{cases},$$

where $\overline{\mu}$ is the effective shear modulus of the composite material under small quasistatic deformations. From work[22] on suspensions

of rigid inclusions in rubber, we know that the same conjecture cannot possibly hold in space dimension $n = 3$. However, from the same and ensuing works,[47–49] we also know that for $n = 3$ the homogenized behavior of an isotropic hyperelastic material comprised of incompressible Neo-Hookean elastomers is, in essence, Neo-Hookean—that is, the resulting effective stored-energy function is approximately linear in $\overline{I}_1 = \overline{\mathbf{F}}\cdot\overline{\mathbf{F}}$ and independent of $\overline{I}_2 = \overline{\mathbf{F}}^{-1}\cdot\overline{\mathbf{F}}^{-1}$.

Interestingly, Ghosh and Lopez-Pamies[6] have shown that the above behavior remains true in the more general setting of an isotropic incompressible Neo-Hookean elastomer filled with incompressible liquid inclusions that are separated from the elastomer by interfaces featuring a constant initial surface tension. This implies that the formula (33) can be used not only to characterize the macroscopic mechanical response of a random isotropic suspension of liquid n-spherical inclusions in an isotropic incompressible elastomer under small quasistatic deformations, but also under moderately large quasistatic deformations (when the elasticity of the elastomer may be approximated as Neo-Hookean). Precisely, we have that the macroscopic or homogenized mechanical response of a random isotropic suspension of liquid n-spherical inclusions, each having identical initial radius A, in an isotropic incompressible elastomer subjected to finite quasistatic deformations is hyperelastic and that its effective stored-energy function is given approximately by

$$\overline{W}(\overline{\mathbf{F}}) = \begin{cases} \dfrac{\overline{\mu}_n}{2}\left[\overline{\mathbf{F}}\cdot\overline{\mathbf{F}} - n\right] & \text{if } \det\overline{\mathbf{F}} = 1 \\ +\infty & \text{else} \end{cases}, \quad n = 2, 3,$$

where the effective shear modulus $\overline{\mu}_n$ is given by the proposed formula (33).

Conflicts of interest

There are no conflicts to declare.

Appendices

Appendix A. The effective shear modulus of a hexagonal suspension of monodisperse liquid 2-spheres

In this appendix, we present numerical solutions for the effective shear modulus $\overline{\mu}_2^{\text{Hex}}$ of a hexagonal suspension of monodisperse liquid 2-spherical inclusions. They are generated by solving—*via* the same FE scheme utilized in Section 4—the unit-cell problem (14) over the pertinent unit cells $\mathscr{Y}$ and then computing the resulting effective modulus of elasticity (13). The calculations are performed over the ranges eCa $\in$ [0,10] and $c \in$ [0,0.905] of elasto-capillary numbers and volume fractions of inclusions. For illustration purposes, Fig. 6 shows two of the unit cells used for $c = 0.6$ and $c = 0.905$.

Much like random isotropic suspensions, hexagonal suspensions also lead to a macroscopic elastic response that is isotropic. In particular, if the elastomer and the liquid making up the inclusions are both incompressible, the effective modulus of elasticity is of the isotropic incompressible form

$$\overline{\mathbf{L}} = 2\overline{\mu}_2^{\text{Hex}}\mathbb{K} + \infty\mathbb{J}$$

Fig. 6 Unit cells $\mathscr{Y}$ for hexagonal suspensions of monodisperse liquid 2-spherical inclusions of radius A at volume fractions (a) $c = 0.6$ and (b) $c = 0.905$.

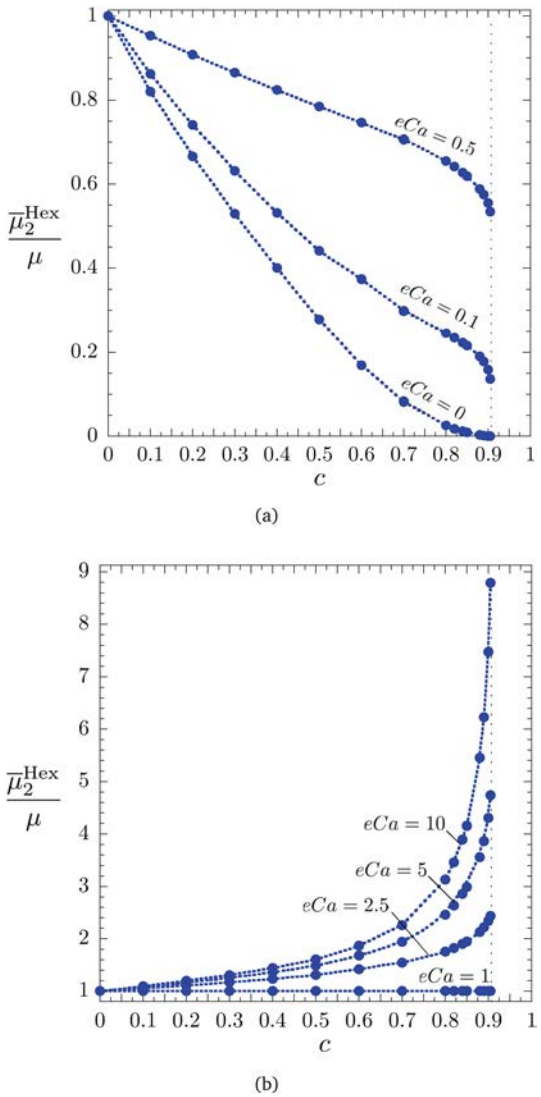

Fig. 7 Finite-element results for the effective shear modulus $\overline{\mu}_2^{\text{Hex}}$ of a hexagonal suspension of monodisperse liquid 2-spherical inclusions in an isotropic incompressible elastomer. The results are shown normalized by the shear modulus μ of the elastomer as a function of the volume fraction c of inclusions for elasto-capillary numbers $0 \leq$ eCa < 1 in part (a) and for eCa ≥ 1 in part (b).

Fig. 7 presents the FE solutions obtained for the normalized effective shear modulus $\overline{\mu}_2^{\mathrm{Hex}}/\mu$ as a function of the volume fraction c of inclusions for seven different values of elasto-capillary number, eCa = 0, 0.1, 0.5, 1, 2.5, 5, 10. Part (a) of the figure shows the results for $0 \leq \mathrm{eCa} < 1$, while part (b) shows the results for $\mathrm{eCa} \geq 1$.

In order to estimate the effective shear modulus at percolation $\overline{\mu}_2^{\mathrm{Hex,perc}}$, one can extrapolate the data in Fig. 7 from $c = 0.905$ to the percolation threshold $c = \pi/2\sqrt{3} \approx 0.9069$. The result obtained is given by relation (23) in the main body of the text.

Appendix B. The two effective shear moduli of a body-centered cubic suspension of monodisperse liquid 3-spheres

Finally, in this appendix, we present numerical solutions for the effective modulus of elasticity $\overline{\mathbf{L}}$ of a BCC suspension of monodisperse liquid 3-spherical inclusions. They are generated by solving—*via* the same FE scheme utilized in Section 4—the unit-cell problem (14) over the pertinent unit cells $\mathscr{Y}$ and then computing the resulting effective modulus of elasticity (13). The calculations are performed over the ranges $\mathrm{eCa} \in [0,10]$ and $c \in [0,0.675]$ of elasto-capillary numbers and volume fractions of inclusions. For illustration purposes, Fig. 8 shows two of the unit cells used for $c = 0.3$ and $c = 0.67$.

In contrast to random isotropic suspensions, BCC suspensions lead not to a macroscopic elastic response that is isotropic, but to one with cubic symmetry. In particular, if the elastomer and the liquid making up the inclusions are both incompressible, the effective modulus of elasticity is of the cubic incompressible form

$$\overline{\mathbf{L}} = 2\overline{\mu}_3^{\mathrm{BCC_a}}\mathbb{K}_{\mathrm{a}} + 2\overline{\mu}_3^{\mathrm{BCC_s}}\mathbb{K}_{\mathrm{s}} + \infty\mathbb{J},$$

where $\mathbb{K}_{\mathrm{a}} = \mathbb{S} - \mathbb{J}$, $\mathbb{K}_{\mathrm{s}} = \mathbb{K} - \mathbb{K}_{\mathrm{a}}$, and

$$\mathbb{S}_{ijkl} = \begin{cases} 1 & \text{if } i = j = k = l \\ 0 & \text{else} \end{cases}$$

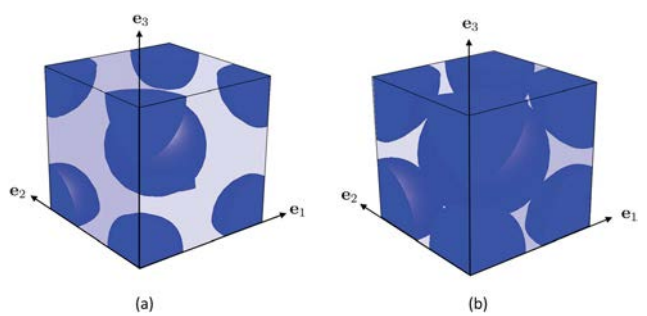

Fig. 8 Unit cells $\mathscr{Y}$ for BCC suspensions of monodisperse liquid 3-spherical inclusions of radius A at volume fractions (a) $c = 0.3$ and (b) $c = 0.67$.

when the laboratory Cartesian frame of reference $\{\mathbf{e}_i\}$ is chosen to coincide with the principal axes of the cubic symmetry of the suspension; see Fig. 8.

Fig. 9 and 10 present, respectively, the FE solutions obtained for the normalized effective axisymmetric shear modulus $\overline{\mu}_3^{\mathrm{BCC_s}}/\mu$ and effective simple shear modulus $\overline{\mu}_3^{\mathrm{BCC_a}}/\mu$ as functions of the volume fraction c of inclusions for seven different values of elasto-capillary number, eCa = 0, 0.1, 0.5, 1, 2.5, 5, 10. Parts (a) of the figures show the results for $0 \leq \mathrm{eCa} < 1$, while parts (b) show the results for $\mathrm{eCa} \geq 1$.

In order to estimate the effective shear moduli at percolation $\overline{\mu}_2^{\mathrm{BCC_a,perc}}$ and $\overline{\mu}_2^{\mathrm{BCC_s,perc}}$, once again, one can extrapolate the data in Fig. 9 and 10 from $c = 0.675$ to the percolation threshold

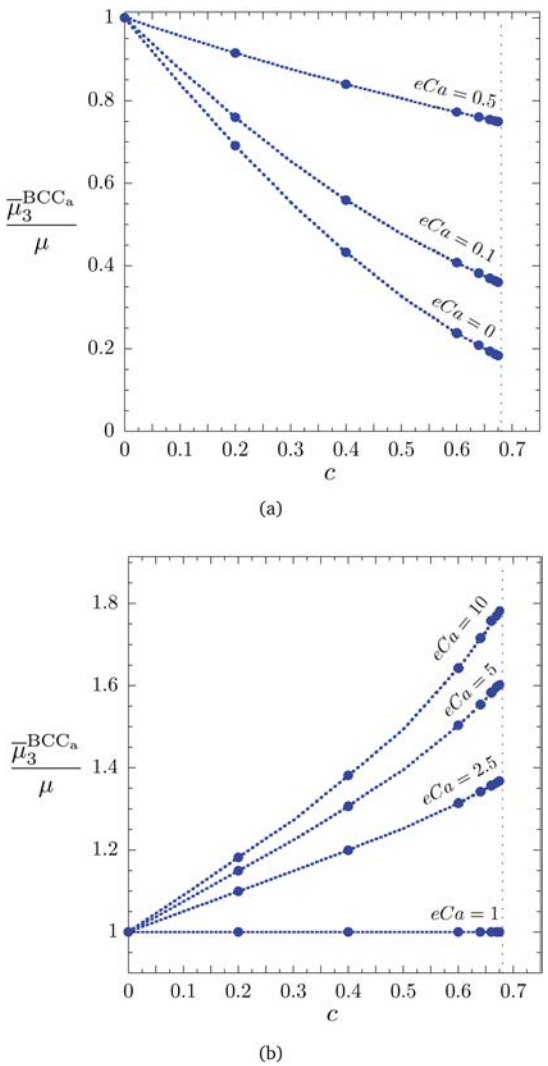

Fig. 9 Finite-element results for the effective axisymmetric shear modulus $\overline{\mu}_3^{\mathrm{BCC_a}}$ of a BCC suspension of monodisperse liquid 3-spherical inclusions in an isotropic incompressible elastomer. The results are shown normalized by the shear modulus μ of the elastomer as a function of the volume fraction c of inclusions for elasto-capillary numbers $0 \leq \mathrm{eCa} < 1$ in part (a) and for $\mathrm{eCa} \geq 1$ in part (b).

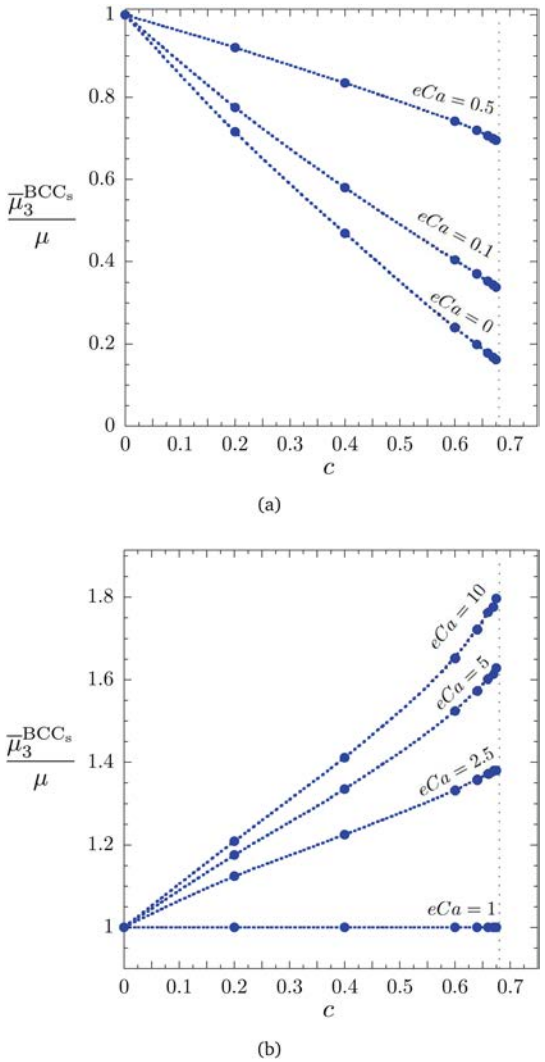

Fig. 10 Finite-element results for the effective simple shear modulus $\overline{\mu}_3^{\mathrm{BCC_s}}$ of a BCC suspension of monodisperse liquid 3-spherical inclusions in an isotropic incompressible elastomer. The results are shown normalized by the shear modulus μ of the elastomer as a function of the volume fraction c of inclusions for elasto-capillary numbers $0 \leq \mathrm{eCa} < 1$ in part (a) and for $\mathrm{eCa} \geq 1$ in part (b).

$c = \sqrt{3}\pi/8 \approx 0.6802$. The results obtained are given by relations (26) and (27) in the main body of the text.

Acknowledgements

Support for this work by the National Science Foundation through the Grant DMREF-1922371 is gratefully acknowledged.

Notes and references

1 O. Lopez-Pamies, *J. Mech. Phys. Solids*, 2014, **64**, 61–82.
2 R. W. Style, R. Boltyanskiy, A. Benjamin, K. E. Jensen, H. P. Foote, J. S. Wettlaufer and E. R. Dufresne, *Nat. Phys.*, 2015, **11**, 82–87.
3 M. D. Bartlett, N. Kazem, M. J. Powell-Palm, X. Huang, W. Sun, J. A. Malen and C. Majidi, *Proc. Natl. Acad. Sci. U. S. A.*, 2017, **114**, 2143–2148.
4 V. Lefèvre, K. Danas and O. Lopez-Pamies, *J. Mech. Phys. Solids*, 2017, **107**, 343–364.
5 G. Yun, S. Y. Tang, S. Sun, D. Yuan, Q. Zhao, L. Deng, S. Yan, H. Du, M. D. Dickey and W. Li, *Nat. Commun.*, 2019, **10**, 1300.
6 K. Ghosh and O. Lopez-Pamies, *J. Mech. Phys. Solids*, 2022, **166**, 104930.
7 K. Ghosh, V. Lefèvre and O. Lopez-Pamies, *arXiv*, 2022, preprint, arXiv.2207.09754, DOI: 10.48550/arXiv.2207.09754.
8 H. S. M. Coxeter, *Regular Polytopes*, Dover, Mineola, NY, 1973.
9 V. Lefèvre and O. Lopez-Pamies, *Extreme Mech. Lett.*, 2022, **55**, 101818.
10 R. W. Style, J. S. Wettlaufer and E. R. Dufresne, *Soft Matter*, 2015, **11**, 672–679.
11 F. Mancarella, R. W. Style and J. S. Wettlaufer, *Soft Matter*, 2016, **12**, 2744–2750.
12 F. Mancarella, R. W. Style and J. S. Wettlaufer, *Proc. R. Soc. London, Ser. A*, 2016, **472**, 20150853.
13 S. Krichen, L. Liu and P. Sharma, *J. Mech. Phys. Solids*, 2019, **127**, 332–357.
14 J. D. Eshelby, *Proc. R. Soc. London, Ser. A*, 1967, **241**, 376–396.
15 Z. Hashin and S. Shtrikman, *J. Mech. Phys. Solids*, 1963, **11**, 127–140.
16 R. M. Christensen and K. M. Lo, *J. Mech. Phys. Solids*, 1979, **27**, 315–330.
17 A. Bensoussan, J. L. Lions and G. Papanicolau, *Asymptotic Analysis for Periodic Structures*, AMS, Chelsea, Providence, 2011.
18 G. D. Scott, *Nature*, 1960, **188**, 908–909.
19 B. D. Lubachevsky and F. H. Stillinger, *J. Stat. Phys.*, 1990, **60**, 561–583.
20 B. D. Lubachevsky, F. H. Stillinger and E. N. Pinson, *J. Stat. Phys.*, 1991, **64**, 501–523.
21 A. A. Gusev, *J. Mech. Phys. Solids*, 1997, **45**, 1449–1459.
22 O. Lopez-Pamies, T. Goudarzi and K. Danas, *J. Mech. Phys. Solids*, 2013, **61**, 19–37.
23 V. Lefèvre, G. A. Francfort and O. Lopez-Pamies, *J. Elasticity*, 2022, **149**, 1–8.
24 A. E. H. Love, *A Treatise on the Mathematical Theory of Elasticity*, Cambridge University Press, Cambridge, UK, 1906.
25 G. I. Taylor, *Proc. R. Soc. London, Ser. A*, 1932, **138**, 41–48.
26 J. M. Peterson and M. Fixman, *J. Chem. Phys.*, 1963, **39**, 2516–2523.
27 G. D. Batchelor and J. T. Green, *J. Fluid Mech.*, 1972, **56**, 401–427.
28 J. R. Willis and J. R. Acton, *Q. J. Mech. Appl. Math.*, 1976, **29**, 163–177.
29 H. S. Chen and A. Acrivos, *Int. J. Solids Struct.*, 1978, **14**, 349–364.
30 M. Duerinckx and A. Gloria, arXiv:2008.03837, 2021.
31 H. M. Princen, *J. Colloid Interface Sci.*, 1983, **91**, 160–175.
32 J. D. Bernal and J. Mason, *Nature*, 1960, **188**, 910–911.

33 B. V. Derjaguin, *Kolloid-Z*, 1933, **64**, 1–6.
34 D. Stamenovic and T. A. Wilson, *J. Appl. Mech.*, 1984, **51**, 229–231.
35 H. M. Princen and A. D. Kiss, *J. Colloid Interface Sci.*, 1986, **112**, 427–437.
36 B. Budiansky and E. Kimmel, *J. Appl. Mech.*, 1991, **58**, 289–290.
37 D. Stamenovic, *J. Colloid Interface Sci.*, 1991, **145**, 255–259.
38 T. G. Mason, J. Bibette and D. A. Weitz, *Phys. Rev. Lett.*, 1995, **75**, 2051–2054.
39 G. C. Papanicolaou and S. R. S. Varadhan, *Colloquia Mathematica Societatis János Bolyai*, 1981, vol. **27**, pp. 835–873.
40 D. Bruggeman, *Ann. Phys.*, 1935, **416**, 636–664.
41 R. Roscoe, *Rheol. Acta*, 1973, **12**, 404–411.
42 H. Eilers, *Kolloid-Z.*, 1941, **97**, 313–321.
43 R. Rutgers, *Rheol. Acta*, 1962, **2**, 305–348.
44 J. J. Stickel and R. L. Powell, *Annu. Rev. Fluid Mech.*, 2005, **37**, 129–149.
45 A. Norris, *Mech. Mater.*, 1985, **4**, 1–16.
46 M. Avellaneda, *Commun. Pur. Appl. Math.*, 1987, **40**, 527–554.
47 T. Goudarzi, D. W. Spring, G. H. Paulino and O. Lopez-Pamies, *J. Mech. Phys. Solids*, 2015, **80**, 37–67.
48 V. Lefèvre and O. Lopez-Pamies, *J. Mech. Phys. Solids*, 2017, **99**, 409–437.
49 V. Lefèvre and O. Lopez-Pamies, *J. Mech. Phys. Solids*, 2017, **99**, 438–470.

